HUMBOLDT-UNIVERSITÄT ZU BERLIN

LEBENSWISSENSCHAFTLICHE FAKULTÄT
INSTITUT FÜR BIOLOGIE

MASTERARBEIT

ZUM ERWERB DES AKADEMISCHEN GRADES MASTER OF SCIENCE

„Visualisierung der Aktivierung des mitotischen Checkpoints in Bäckerhefe mithilfe von YFP-markiertem Mad2“

„Visualization of Spindle Assembly Checkpoint Activation in Budding Yeast Using YFP-Tagged Mad2“

vorgelegt von Wiebke Schmidt
geb. am 15.09.1990 in Demmin

angefertigt im Banfield Laboratory, Division of Life Science
Hong Kong University of Science and Technology, SAR Hongkong

Berlin, im Dezember 2017

Zusammenfassung

Während der Zellteilung verhindert die Aktivierung des mitotische Checkpoints den Übergang der Zelle in die Anaphase, sollten einzelnde Kinetochore nicht an den mitotischen Spindelapparat angeheftet sein. Die Rekrutierung des Proteins Mad2 von der Zellkernhülle zu diesen Kinetochoren ist notwendig für die Aktivierung des Checkpoints (De Antoni et al., 2005). Durch Markierung von Mad2 mit fluoreszierendem Protein wird die Verlagerung beobachtbar (Iouk et al., 2002). In der vorliegenden Arbeit wurde untersucht, inwieweit sich mit gelb fluoreszierendem Protein (YFP, engl. *yellow fluorescent protein*) markiertes Mad2 dazu eignet, den AN/AUS-Status des Checkpoints in der Hefe *Saccharomyces cerevisiae* auf Einzelzellebene zu visualisieren. Ziel war die Entwicklung eines Checkpoint Markers, der wertvolle Hinweise über den Zellzustand von z. B. genmanipulieren Zelllinien geben könnte.

Es konnte gezeigt werden, dass sich markiertes Mad2 nicht als Reporter der Checkpoint Aktivität eignet, da vermutlich die Menge des gebundenen Proteins pro Kinetochor zu gering ist, um ein aussagekräftiges und zuverlässiges fluoreszentes Signal zu generieren. Dennoch konnte durch die Verwendung von Split-GFP ein vielversprechender Ansatz für zukünftige Arbeiten auf diesem Gebiet gefunden werden.

Abstract

During the cell cycle, activation of spindle assembly checkpoint prevents anaphase transition in case of unattached kinetochores. The recruitment of Mad2 from nuclear envelope to those kinetochores is essential for checkpoint activation (De Antoni et al., 2005). Previous studies showed that tagging of Mad2 with fluorescent protein can make the location shift visible (Iouk et al., 2002). It is the objective of the present study to examine the suitability of yellow fluorescent protein (YFP) tagged Mad2 to visualize the ON/OFF status of the checkpoint in *Saccharomyces cerevisiae* on single cell level. The aim is to develop a checkpoint marker that provides essential information about the cell status of for example mutant strains.

The study demonstrates that tagged Mad2 is inappropriate to monitor the checkpoint status. The reason for that may be the insufficient amount of Mad2 bound to a single kinetochore. Nevertheless, utilizing split-GFP was found as a promising method for further studies.

Table of Contents

List of figures

List of Tables

List of Abbreviations

AmpR	*bla* marker
APS	Ammonium persulfate
ARS	Autonomously replicating sequence
Bet1	Golgi vesicular membrane trafficking protein
BSA	Bovine serum albumin
C-Mad2	Closed conformation of Mad2
Cdc20	Cell-division cycle protein 20
CEN	Centromere sequence
CENIV	Chromosome IV centromere DNA
ChIP	Chromatin immunoprecipitation
CIP	Alkaline phosphatase, calf intestinal
CMK	Cytidylate kinase
ConA	Concanavalin A
DAPI	4',6-diamidino-2-phenylindole
ddH_2O	Double distilled water
DMSO	Dimethyl sulfoxide
DNA	Deoxyribonucleic acid
dNTP	deoxyribose nucleoside triphosphate
DTT	Dithiothreitol
ECitrine	Enhanced Citrine
ECL	Electrochemiluminescence
EDTA	Ethylenediaminetetraacetic acid
EmCit	Enhanced monomeric Citrine
G418	Geneticin
GAGA	Glycine-Alanine (2x) sequence
GC	Guanine-cytosine
GFP	Green fluorescence protein
HF	High fidelity
I-Mad2	Intermediate conformation of Mad2
Kb	Kilobase
LB	Lysogeny broth
LEU	Leucine
LioAc	Lithium acetate
loxP	locus of X-over P1
Mad2	Mitotic arrest deficient 2
MCC	Mitotic checkpoint complex

MTOC	Microtubule organizing center
NaOH	Sodium hydroxide
NC	Negative control
NPC	Nuclear pore complexes
O-Mad2	Open conformation of Mad2
OD	Optical density
PAGE	Polyacrylamide gel electrophoresis
PBS	Phosphate buffered saline
PBST	Phosphate buffered saline tween-20
PC	Positive control
PCR	Polymerase chain reaction
PEG	Polyethylene glycol
PI	Protease inhibitor
rpm	Rounds per minute
SAC	Spindle assembly checkpoint
SB	Sample buffer
SDS	Sodium dodecyl sulfate
SPB	Spindle pole bodies
ssDNA	Single-stranded DNA
T_a	Annealing temperature
TAE	Tris-acetate-EDTA
TE	Tris and EDTA buffer
TEMED	Tetramethylethylenediamine
T_m	Melting temperature
Tris	Tris(hydroxymethyl)aminomethane
Tris-HCl	Tris hydrochloride buffer
Ts	Temperature sensitive
U	Unit
WT	wild type
YCp	Yeast centromere plasmid
YEPD	Yeast extract peptone dextrose
YFP	Yellow fluorescent protein

1 Introduction

The unicellular yeast *Saccharomyces cerevisiae* is a popular model organism for higher eukaryotes and cell cycle regulation. By studying the yeast cell cycle, fundamental properties of life like growth and proliferation can be examined. The cell cycle, depicted in Figure 1, is a succession of events whereby a cell grows and divides into two daughter cells. It consists of DNA replication in synthesis phase (S) and sister chromatid separation in mitotic phase (M). S and M phases are separated by gap phases (G_1, G_2). Additionally, M phase is divided into prometaphase, anaphase and telophase/cytokinesis.

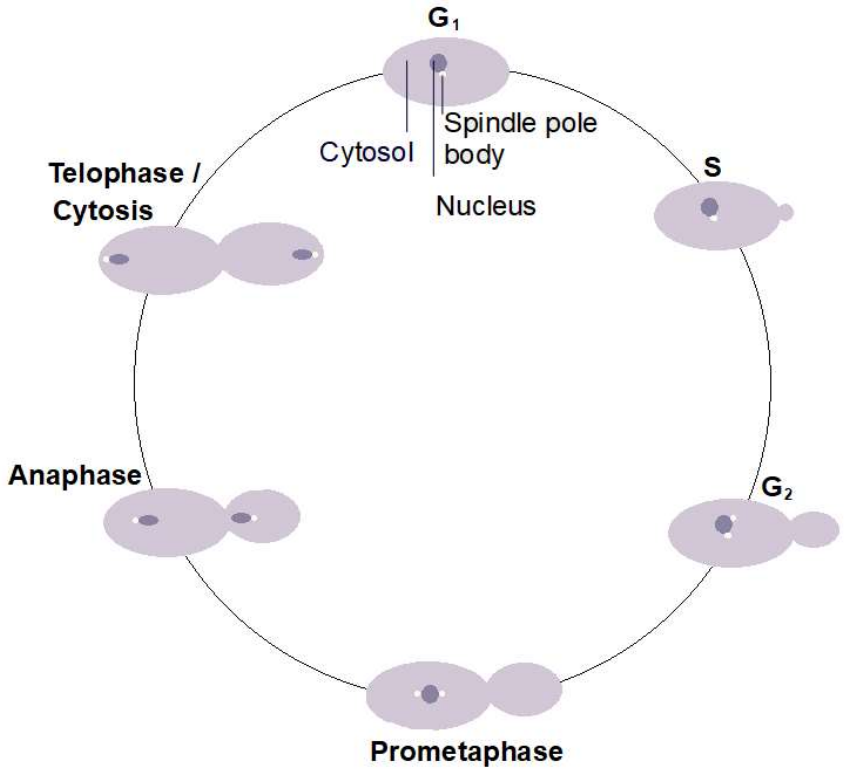

Figure 1: Cell cycle of budding yeast. Phases of the cell cycle are depicted in a clockwise direction. Cell growth happens in G_1 phase, followed by DNA replication in S. Interphase ends with G_2. Sister chromatid separation and cell division take place in mitotic phase (M). M consists of prometaphase, anaphase and telophase/cytokinesis.

During cells cycle progress, cells pass two significant checkpoints: the G_1 checkpoint and the spindle assembly checkpoint (SAC). Activation of one of these checkpoints cause cell cycle arrest in either G_1 phase or M phase.

1.1 Separation of sister chromatids and M phase transition

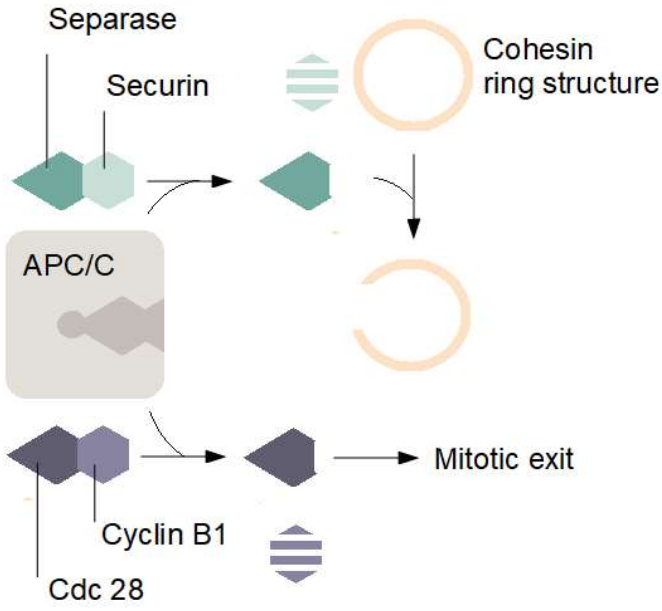

Figure 2: Role of the anaphase-promoting complex (APC/C) in chromosome segregation. Protein degradation of securin and cyclin B1 by APC/C triggers anaphase. Separase hydrolyzes the cohesin ring structure, a protein structure responsible for binding sister chromatids. Degradation of Cdc28-cyclin B1 complex leads to the destruction of M cyclins (e.g., Clb 1-4), which allows mitotic exit. (Own diagram based on Lara-Gonzalez et al., 2012)

At the beginning of M phase, the mitotic spindle moves the chromosomes to opposite poles. An inaccurate chromosome segregation can lead to aneuploidy, which can result in growth defects or cell death (Mulla et al., 2014). A multi-protein structure called kinetochore mediates the interaction between mitotic spindle and chromosomes (Cheeseman and Desai, 2008; Westermann et al., 2007). The spindle pole bodies (SPB)

play a crucial role in assembly of the mitotic spindle and serve as microtubule organizing centers (MTOCs) (Meyer et al., 2013). In mitotic cells, the SPB sit at the opposite poles and attach to the kinetochores by microtubules. To avoid segregation defects, cells need to ensure that all kinetochores are bound by microtubules before the metaphase-to-anaphase transition. The phase transition is regulated by the E3 ubiquitin ligase anaphase-promoting complex (APC/C) (Pines, 2011) (Figure 2). The APC/C is a large complex of 11–13 subunits and targets cell cycle proteins for degradation by the 26S proteasome. As shown in Figure 2, degradation of securin by APC/C releases the cysteine protease separase. Separase hydrolyzes cohesin, which is responsible for binding sister chromatids in early stages of the anaphase (Nasmyth and Haering, 2009). Cleavage of cohesin leads to separation of the sister chromatids (Uhlmann et al., 2000). Another target of APC/C is the regulatory protein cyclin B1. It forms a complex with Cdc28 (cyclin-dependent kinase 1) and is involved in early events of mitosis (Gorr et al., 2005). At the end of mitosis, the APC/C targets cyclin B1 for degradation which allows mitotic exit.

1.2 Activation of spindle assembly checkpoint

Since unequal chromosome distribution leads to serious damage, all sister chromatids need to be correctly attached to microtubules of the SPB before committing segregation. Unattached kinetochores initiate a signals cascade which prevents anaphase until all chromatids are bound to microtubules (Rieder et al., 1995). The cell cycle arrest is caused by activation of the mitotic checkpoint or spindle assembly checkpoint (Figure 3). The SAC also maintains active in case of weak tension (Zhou et al., 2002). A proper connection between chromatids and spindle generates tension at the kinetochores. The bi-oriented tension of opposite spindle poles stabilizes the kinetochore-microtubule assembly whereas asymmetrical tension has a destabilizing effect. Destabilization of incorrect attachment allows the kinetochore to reattach correctly to the microtubules of the spindle. To arrest cell cycle progress, the presence of a single kinetochore pair without correct bipolar attachment is sufficient (Rieder et al., 1994; Li and Nicklas, 1995). The SAC activation inhibits APC/C and delays prometaphase. The APC/C inhibition mechanism is poorly understood; however, it is known, that regulation of mitotic checkpoint complex (MCC)

activity plays an important role (Alfieri et al., 2016). It is hypothesized that the MCC binds to APC/C as a pseudosubstrate. Figure 3 shows the mechanism. The spindle assembly checkpoint components MAD2 and MAD3 (which will hereinafter be referred to as Mad2 respectively Mad3), as well as the cell cycle arrest protein BUB3 (hereinafter referred to as Bub3) and the cell division cycle protein 20 (Cdc20), assemble to form the MCC (Figure 3). However, the order of subunit attachment remains unknown. The "MAD2-template model" is the leading model of MCC formation (De Antoni et al., 2005). The spindle assembly checkpoint component MAD1 (hereinafter referred to as Mad1) forms a complex with the closed conformer of Mad2 (C-Mad2) and binds to unattached kinetochores. That complex recruits open Mad2 (O-Mad2), which forms an asymmetric dimer with Mad1 bound C-Mad2 while changing its conformation to the intermediate form of Mad2 (I-Mad2). Mad1 and Cdc20 both contain a similar Mad2-binding motif. In an auto-amplification reaction, I-Mad2 binds Cdc20 and changes conformation to C-Mad2. A Mad3-Bub3 complex binds Cdc20-C-Mad2 for MCC formation. It is believed, that the mitotic checkpoint complex binds to the binding pocket of APC/C as a pseudosubstrate. APC/C cannot target securin or cyclin B1 for degradation, mitotic exit is prolonged (Figure 2).

A mechanism for SAC deactivation may be the energy-dependent dissociation of Mad2-Cdc20, while unattached kinetochores are continuously recreating Mad2-Cdc20 to maintain the SAC active.

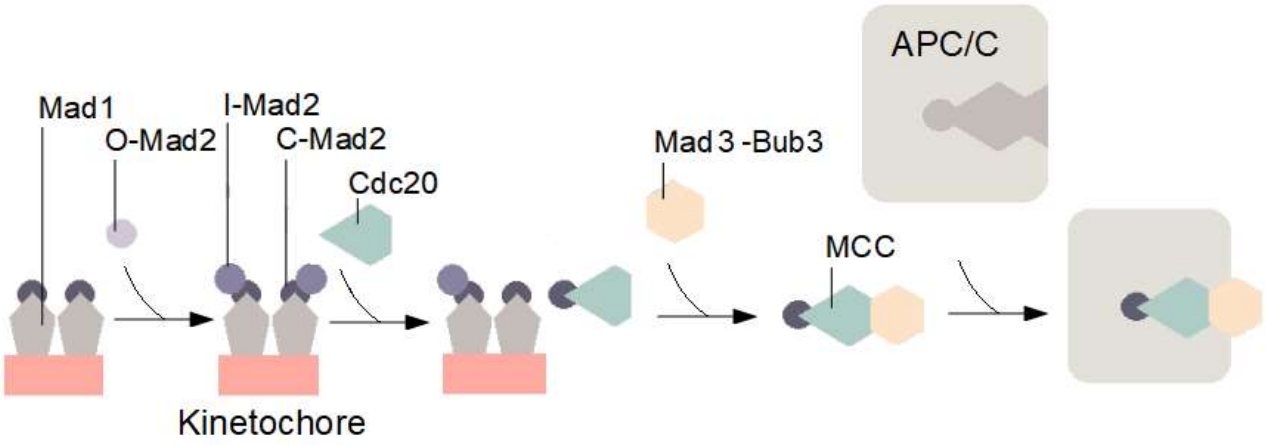

Figure 3: The Mad2-templet-model and blockage of APC/C. Spindle assembly checkpoint activation requires the recruitment of different proteins to unattached kinetochores. Free open Mad2 (O-Mad2) recruited from the nuclear envelope changes its conformation to closed Mad2 (C-Mad2) by binding to a Mad1 dimer. Mad1 bound C-Mad2 can form a heterodimer with another free O-Mad2 by changing its conformation to intermediate Mad2 (I-Mad2). Somehow I-Mad2 then binds to Cdc20 under conformation changes to C-Mad2. A Mad3-Bub3 complex binds to Cdc20-Mad2 to form the mitotic checkpoint complex (MCC). However, the order of attachment to form the MCC remains unknown. It is hypothesized, that the complex blocks the binding pocket of APC/C and delays the progress of the cell cycle. (Own diagram based on Lara-Gonzalez et al., 2012)

1.3 The mitotic Mad2 protein

The mitotic arrest defective (MAD) genes 1-3 were first identified in budding yeast (Li and Murray, 1991). Mad2 is necessary for SAC activation since it forms the seed of the mitotic checkpoint complex along with Cdc20. The protein has at least three different conformations which differ in the positioning of the C-terminal segment, called “safety belt” (Figure 4a) (Hara et al., 2015). In the open and intermediate form of Mad2, this residue is held close to the protein. C-Mad2 bound to either Mad1 or Cdc20 wraps the safety belt around the ligand. Thus, the belt interacts with a different region of Mad2.

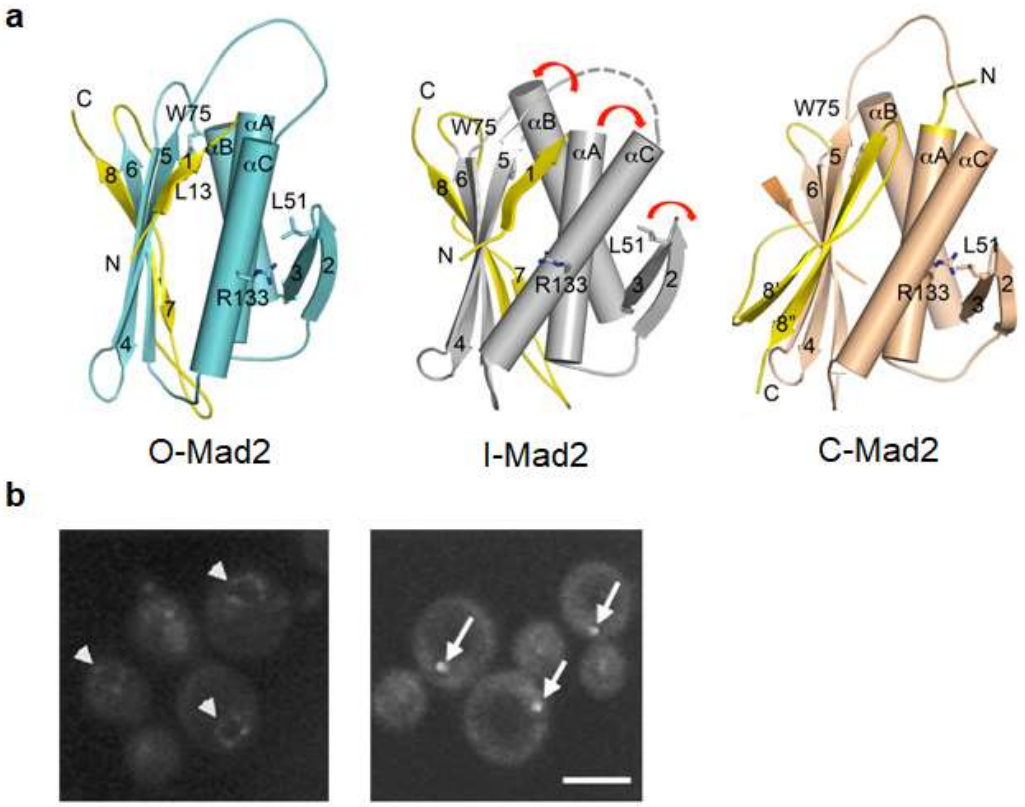

Figure 4: Conformation and location changes of Mad2. (a) Predictions of O-Mad2, I-Mad2 and C-Mad2. The C-terminal segment ("safety belt", top left of the structure) is held close to the protein in O-Mad2 and I-Mad2. C-Mad2 wraps the safety belt around the ligand (bottom left) (from Hara et al., 2015). (b) Microscopic images of Mad2-GFP in budding yeast. Mad2-GFP in cycling cells (left) shows the pattern of the nuclear envelope. The protein is located at the NCPs. After nocodazole treatment (right) Mad2-GFP is recruited to kinetochores for SAC activation. A clear kinetochore signal is visible. Bar: 5 µm (from Iouk et al., 2002).

Mad2 and Mad1 are both associated with the NPCs of *S. cerevisiae* in cycling cells (Iouk et al., 2002). SAC activation requires the recruitment of both proteins to unattached kinetochores. Although the C-terminus is responsible for Mad2 conformation changes, it was successfully tagged with green fluorescent protein (GFP) in previous studies. Depicted in Figure 4b is the location shift of Mad2-GFP from the nuclear envelope (left) to

the kinetochores (right) of nocodazole-treated cells (Iouk et al., 2002). The drug enhances microtubule polymerization which leads to a delay in kinetochore attachment.

1.4 The GFP variant EmCitrine

Tagging cassettes like GFP can be fused to a target protein under the control of its native promoter. Since the expression level is often low, fluorescence tagged proteins can be difficult to detect. Codon optimization can improve the expression of fluorescent protein fusions. Therefore, sequences of fluorescent proteins were optimized to use the most abundant codons of a particular organism. One of the codon-optimized GFP variants is the improved yellow fluorescent protein (YFP) Citrine. Citrine is more resistant than YFP. Thus, it has an increased photostability and folding efficiency (Griesbeck et al., 2001; Miyawaki et al., 1999). Enhanced Citrine (ECitrine) is about twice as detectable as unoptimized YFP. Further optimization of ECitrine was carried out by the creation of a monomeric version (EmCitrine). Usually, GFP variants dimerize, which can lead to difficulties when interacting proteins are tagged with GFP variants. In EmCitrine, the dissociation constant was increased by a factor of 1000 due to the introduction of the A206R mutation (Sheff and Thorn, 2004). Because of the high sequence identity of GFP variants, an anti-GFP antibody can detect EmCitine with equal affinity as GFP (Sheff and Thorn, 2004). EmCitrine will be used as tagging cassette in this study.

1.5 Aim of study

Probably the most important contribution of yeast could be the association of genes and proteins with their function. Mutations can be introduced into the yeast genome, and by observing any differences in growth or physiology of mutants to wild type cells, it is possible to study the biochemical function of gene products and consequences of failure in gene function.

As described in paragraph 1.3, Mad2-GFP shift its location at the beginning of SAC activation. Therefore fluorescent tagged Mad2 could be used to monitor the SAC as ON or OFF by visible relocation of the fluorescence signal from nuclear envelope (OFF) to kinetochores (ON). In this study, I would like to examine the suitability of EmCitrine tagged Mad2 as a tool for visualization of checkpoint activity on single cell level. Information about SAC activity could be a gain of knowledge in functional genomics and systems biology. It could help to identify the reason behind different observations such as growth defects or drug sensibilities in mutants and wild type cells.

2 Materials and methods

2.1 Materials

2.1.1 Reagents

Reagent	Manufacture
1 kb plus DNA ladder	Thermo Fisher Scientific, Waltham
10X PCR Buffer (Mg2+ free)	Takara Bio Inc., Kyoto
10X T4 DNA Ligase Buffer	New England Biolabs, Ipswich
4',6-diamidino-2-phenylindole (DAPI)	Sigma-Aldrich, St. Louis
5X Q5 High GC Enhancer	New England Biolabs, Ipswich
5X Q5 Reaction Buffer	New England Biolabs, Ipswich
Acetic Acid	Merck Group, Darmstadt
Acid-washed glass beads	Sigma-Aldrich, St. Louis
Acrylamide	Thermo Fisher Scientific, Waltham
Adenine	Sigma-Aldrich, St. Louis
Adenine hemisulfate salt	Sigma-Aldrich, St. Louis
Alkaline Phosphatase, Calf Intestinal (CIP)	New England Biolabs, Ipswich
Ammonium Persulfate (APS)	Thermo Fisher Scientific, Waltham
Ammonium Sulfate	Becton, Dickinson and Company, Franklin Lakes
Ampicillin	Roche Diagnostics International AG, Rotkreuz
Arginine	Sigma-Aldrich, St. Louis
Aspartic acid	Sigma-Aldrich, St. Louis
BamHI	New England Biolabs, Ipswich
BenchMark prestained Protein Ladder	Thermo Fisher Scientific, Waltham
Benomyl	Sigma-Aldrich, St. Louis
Bovine serum albumin (BSA)	New England Biolabs, Ipswich
Bromophenol Blue	Merck Group, Darmstadt

Concanavalin A	Sigma-Aldrich, St. Louis
CutSmart® Buffer	New England Biolabs, Ipswich
CutSmart® Buffer	New England Biolabs, Ipswich
D-(+)- Glucose Anhydrous	Honeywell Specialty Chemicals Seelze, Seelze
Dimethyl sulfoxide (DMSO)	Sigma-Aldrich, St. Louis
Dithiothreitol (DTT)	Thermo Fisher Scientific, Waltham
dNTP Mixture	Takara Bio Inc., Kyoto
ECL Western Blotting Detection Reagents	GE Healthcare, Illinois
Ethanol, Absolute	Merck Group, Darmstadt
FavorPrep™ Gel/ PCR Purification Kit	Favorgen Biotech Corp.
Ficoll PM400	Sigma-Aldrich, St. Louis
Glutamic acid	Sigma-Aldrich, St. Louis
Glycerol	Sigma-Aldrich, St. Louis
Glycerol	Sigma-Aldrich, St. Louis
Histidine	Sigma-Aldrich, St. Louis
Invitrogen UltraPure Agarose	Thermo Fisher Scientific, Waltham
Invitrogen UltraPure EDTA	Thermo Fisher Scientific, Waltham
Leucine	Sigma-Aldrich, St. Louis
Lysine	Sigma-Aldrich, St. Louis
Methanol	Scharlab, S.L., Barcelona
Methionine	Sigma-Aldrich, St. Louis
Mini Plus Plasmid DNA Extraction System	Viogene BioTek Corp.
NEBuffer	New England Biolabs, Ipswich
NEBuffer 2	New England Biolabs, Ipswich
NEBuffer 3.1	New England Biolabs, Ipswich
NotI	New England Biolabs, Ipswich
NotI-HF®	New England Biolabs, Ipswich
Pefabloc® SC	Sigma-Aldrich, St. Louis
Peptone, Bacteriological	Trafalgar Scientific Ltd, Leicester
Phenol:Chloroform:Isoamyl Alcohol	Merck Group, Darmstadt
Phenylalanine	Sigma-Aldrich, St. Louis
Polyethylene Glycol (3350)	Sigma-Aldrich, St. Louis

Polyethylene Glycol (4000)	Honeywell Specialty Chemicals Seelze, Seelze
Ponceau S	Sigma-Aldrich, St. Louis
Q5® High-Fidelity DNA Polymerase	New England Biolabs, Ipswich
SacII	New England Biolabs, Ipswich
SalI	New England Biolabs, Ipswich
Serine	Sigma-Aldrich, St. Louis
Sodium Acetate 3-hydrate	Merck Group, Darmstadt
Sodium Hydroxide	Honeywell Specialty Chemicals Seelze, Seelze
Sybr® Safe DNA Gel Stain	Thermo Fisher Scientific, Waltham
T4 Ligase	New England Biolabs, Ipswich
TaKaRa Taq™ DNA Polymerase (250 U)	Takara Bio Inc., Kyoto
Tetramethylethylenediamine (TEMED)	Honeywell Specialty Chemicals Seelze, Seelze
Threonine	Sigma-Aldrich, St. Louis
Triton X-100	Sigma-Aldrich, St. Louis
Trizma® (TRIS base)	Sigma-Aldrich, St. Louis
Tryptone	Trafalgar Scientific Ltd, Leicester
Tryptophan	Sigma-Aldrich, St. Louis
Tyrosine	Sigma-Aldrich, St. Louis
Uracil	Sigma-Aldrich, St. Louis
Valine	Sigma-Aldrich, St. Louis
XhoI	New England Biolabs, Ipswich
Xylene Cyanol FF	Merck Group, Darmstadt
Yeast Extract	Trafalgar Scientific Ltd, Leicester
Yeast Nitrogen Base	Becton, Dickinson and Company, Franklin Lakes

2.1.2 Equipment

Equipment	Designation	Manufacture
Filter paper	Whatman Chromatography sheets	Sigma-Aldrich, St. Louis

Membran	GE Amersham Protran Premium, 0.45um, NC	Thermo Fisher Scientific, Waltham
Camera	SPOT RT Monochrome	Diagnostic Instruments Inc., Sterling Heights
Electrophoresis chamber	HE33 Mini Horizontal Agarose Electrophoresis Unit	Hoefer, Inc. Holliston
Electrophoresis Unit SDS-PAGE	Mighty Small II Deluxe Mini Vertical Electrophoresis Unit	Hoefer, Inc. Holliston
Fume		Morgan and Grundy Ltd, APMG Limited, Manchester, UK
Gel documentation system	AlphaImager HP system	ProteinSimple, San Jose
Illuminator	Intensilight Epi-fluorescence Illuminator	Nikon, Tokyo
Incubator 25°C	Model 2005	Sheldon Manufacturing, Inc. Cornelius
Incubator 30°C		Precision Scientific Instruments, Inc.Buffalo
Incubator 37°C		Precision Scientific Instruments, Inc.Buffalo
Microscope	Eclipse 80i	Nikon, Tokyo
Microscope slides	Multispot Microscope Slides	C.A. Hendley Essex Ltd, Essex
Objektive	Plan Apo VC 100X /1.40 Oil	Nikon, Tokyo
PCR Thermocycler	S lowo TM Thermal Cycler	Bio-Rad Laboratories, Hercules
Photometer	Genesys 10UV system	Thermo Spectronic, Rochester
Power Supply	PS500 XT DC Power Supply	Hoefer, Inc. Holliston
Shaker	InnOva 4900	New Brunswick Scientific, Eppendorf AG Hamburg
Spectrometer	NanoDrop™ 2000 spectrometer	Thermo Fisher Scientific, Waltham
Stirring hotplate	Thermolyne® Nuova™ stirring hotplate	Thermo Fisher Scientific, Waltham
Tabletop centrifuge		Eppendorf AG Hamburg
Tabletop film processor	OPTIMAX	PROTEC GmbH & Co. KG Oberstenfeld

Toploader balance	Sartorius BP toploader balance	Thermo Fisher Scientific, Waltham
Transfer tank	Mighty Small Transfer Tank	Hoefer, Inc. Holliston
Vortex	Barnstead Thermolyne Maxi Mix II Vortex Mixer	Thermo Fisher Scientific, Waltham
Water bath	W28, W14	Grant Instruments, Cambridge

2.1.3 Software

Software	Publisher
ImageJ	Java software
SnapGene® Viewer	GSL Biotech LLC, Chicago
Spot Advanced	SPOT Imaging, Diagnostic Instruments, Inc. Sterling Heights

2.1.4 Bacteria and yeast strains

E. coli **Bacterial strain**

Strain name	Description	Source
CMK603	Phenotypically *ecoK- lacZ*ΔM15 *RECA*+ F+	H. Pelham

S. cerevisiae **Yeast strains**

Strain name	Description	Source
BY4741	*MAT*a *his3Δ1 leu2Δ0 met15Δ0 ura3Δ0*	Euroscarf
Y01392	BY4741, *MAD2::kanMX4*	Euroscarf
Y04453	BY4741, *MAD1::kanMX4*	Euroscarf

SARY3739	Y04208 (BY4741, *vps74::kanMX4* (Euroscarf)), *TED1::cloNAT, vps74(AAA)-pRS416*	Lab Collection
SARY3795	SARY3739*, MAD2::his5* (Cre-loxP)	Lab Collection
SARY4981	Y01392, *kanMX4::MAD2-EmCitrine-KILEU2* (Cre-loxP)	This Study
SARY4983	SARY3795, *his5::MAD2-EmCitrine-KILEU2* (Cre-loxP)	This Study
SARY4985	SARY3795, *his5::MAD2-KILEU2* (Cre-loxP)	This Study

2.1.5 Plasmids

Name	Description	Source
pUG73	*loxP-pKlLEU2-KlLEU2-tKlLEU2-loxP*	Euroscarf
415-gHTB3-EmCit-LEU (LoxP)-3`UTR	*HTB3* tagged with *EmCitrine* and *KILEU2* (Cre-loxP), driven by *HTB3* promoter	Lab Collection
415-NEmCit-gMad1	N-terminal portion *EmCitrine* linked to *MAD1,* driven by *MAD1* promoter	Lab Collection
416-Tc-CEmCit-MAD2	C-terminal portion *EmCitrine* linked to *MAD2,* driven by *TPI* promoter	Lab Collection
415-MAD2	*MAD2* driven by its endogenous promoter	Lab Collection
413-MAD2-EmCit-LEU2	*MAD2* driven by its endogenous promoter, linked with GAGA linker to *EmCitrine* and *KILEU2* (loxP)	This Study
415-MAD2-LEU	*MAD2* driven by its endogenous promoter linked to *KILEU2* (loxP)	This Study

2.1.6 Primers

Name	Sequence
KL-Leu2-R	ATCTCATGGATGATATCC
Linker-EmC-F	GGTGCCGGTGCCATGTCTAAAGGTGAAGAA
LoxP-NotI-F	ACCAGCGGCCGCCGACAACCCTTAATA
LoxP-SacII-R	ACCACCGCGGATCTGATATCACCTA
MAD2-promoter-(500)F/SalI	ACCAGTCGACAATAGCATTAAATTCCGGATT
MAD2-promoter-F	TTGCCTTTAATTTTTTTCTTGCCTTTAATTTTTTTC
MAD2-3UTR(200)R/BamHI	ACCAGGATCCAAGCAAAGTTTGAGTGTCAAA
MAD2-5UTR-XhoI-F	ACCACTCGAGTCGTCTTGAACTCTC
MAD2-EmCit-LoxP-R	ATCTATATTCTTTCTAAACATCGAAAACGAGATTTTTTTG GACTTCCGTCGGATCTGATATCACCTAATAAC
MAD2-linker1(GAGA)	GGCACCGGCACCATATTTATAGCTGACCTG
NEmCit-R-Linker	GGCACCGGCACCTTGTTTGTCAGCC
RG02	GTGTGGAATTGTGAGCGGAT
RG05	AGGGTTTTCCCAGTCACGAC

2.1.7 Media

The following media were prepared as described by Guthrie and Fink and sterilized by autoclaving at 121°C and 15 psi for 20 minutes.

2×TY medium (w/v) 1.6 % tryptone, 1 % yeast extract and 0.5 % NaCl

Lysogeny broth (LB) medium (w/v) 1 % tryptone, 0.5 % yeast extract and 0.5 % NaCl

Solid yeast extract peptone dextrose (YEPD) medium (w/v) 1 % yeast extract, 0.0055 % adenine sulphate, 2 % bactopeptone, 2% glucose and 2 % agar

Solid yeast selective medium (w/v) 0.17 % yeast nitrogen base, 0.5 % ammonium sulphate, 2% glucose, 2 % agar and 0.13 % of an appropriate drop-out powder (Table 1)*

*Drop-out powder lacks one or more amino acids. For example -LEU powder omits leucine but contains all other amino acids listed in table 1. The absence of amino acids was used as a selection marker.

Yeast selective medium (w/v) 0.17 % yeast nitrogen base, 0.5 % ammonium sulphate, 2% glucose and 0.13 % of an appropriate drop-out powder (Table 1)*

YEPD medium (w/v) 1 % yeast extract, 0.0055 % adenine sulphate, 2 % bactopeptone and 2% glucose

Table 1: Composition of drop-out powder for selective yeast media*

amino acid	% (w/v)	amino acid	% (w/v)
adenine	0.25	L-phenylalanine	0.3
L-arginine	0.12	L-serine	2.25
L-aspartic acid	0.6	L-threonine	1.2
L-glutamic acid	0.6	L-tryptophan	0.24
L-histidine	0.12	L-tyrosine	0.18
L-leucine	0.36	L-valine	0.9
L-lysine	0.18	uracil	0.12
L-methionine	0.12		

2.1.8 Buffers and solutions

20 % glucose (stock) (w/v) 20 % glucose in ddH_2O

4',6-diamidino-2-phenylindole (DAPI) stock (w/v) 0.25 % DAPI in ddH_2O

Benomyl stock (w/v) 3 % benomyl in DMSO

Blocking buffer 5 % (w/v) nonfat dry milk in washing buffer

Concanavalin A (ConA) stock (w/v) 1 % ConA in ddH_2O

Gel-loading buffer (6X) (w/v) 0.25 % bromophenol blue, 0.25 % xylene cyanol FF and 15 % Ficoll type 400

Lithium Acetate (1 M) (LioAc) (w/v) 10.2 % LioAc dihydrate in ddH_2O

Lithium Acetate / TE 8.0 (0.1 M) (LioAc TE) 1.02 % (w/v) LioAc dihydrate, 1 % (v/v) Tris-HCl (1 M, pH 8.0) and 0.2 % (v/v) EDTA (0.5 M, pH 8.0)

Phosphate buffered saline (PBS) (w/v) 0.8 % NaCl, 0.02 % KCl, 0.144 % Na_2HPO_4 and 2.4 % KH_2PO_4

Polyethylene Glycol (PEG) 3350 (50 %) (w/v) 50 % PEG 3350 in LioAc TE

Polyethylene glycol (PEG) 4000 (50 %) (w/v) 50 % PEG 4000 in LioAc TE

Running buffer (v/v) 0.2 % running buffer stock (5X) and 0.01 % SDS (10 %)

Running buffer stock (5X) (w/v) 14.4 % glycine and 3 % Tris base

SDS sample buffer stock (2X) (v/v) 16 % Tris (1 M, pH 6.8), 16 % glycerol, 40 % SDS (10 %) and 28 % H_2O. Bromphenol blue was added by instinct.

Sodium dodecyl Sulfate (SDS) (10 %) (w/v) 10 % SDS in ddH_2O

Transfer buffer (v/v) 0.1 % running buffer stock (5X), 0.2 % methanol and 0.002 % SDS (10 %)

Tris-acetate-EDTA (TAE) buffer stock (50X) 24.2 % (w/v) Tris base, 5.71 % (v/v) acetic acid and 10 % (v/v) EDTA (0.5 M pH 8.0)

Tris-HCl (1 M, pH 8.0) 12.11 % (w/v) Tris base and ~4.2 % (v/v) HCl to adjust pH at 8.0

Washing buffer (Phosphate buffered saline tween-20, PBST pH 7.2) 0.8 % (w/v) NaCl, 0.02 % (w/v) KCl, 0.144 % (w/v)Na_2HPO_4, 0.024 % (w/v) KH_2PO_4 and 0.5 % (v/v) tween-20 (20 %)

Yeast lysis buffer 2 % (v/v) Triton X-100, 1 % (w/v) SDS, 0.5844 % (w/v) NaCl, 1 % (v/v) Tris-HCl (1 M, pH 8.0), 0.2 % (v/v) Na2EDTA (500 mM).

2.2 Methods

2.2.1 Molecular biological methods

2.2.1.1 Agarose gel electrophoresis

To separate DNA-fragments of mixed fragment populations (2.2.1.3, 2.2.1.8, 2.2.1.9) a matrix of agarose was used. A 0.8 % (w/v) solution of agar in 1X TAE buffer was cooked at least three times. 5X Sybr® Safe DNA Gel Stain was added after cooling down to ~ 60 °C. The gel was cast into a tray of an electrophoresis chamber. After solidification, 1X gel-loading buffer and DNA samples were mixed and filled into the wells. A 1 Kb DNA ladder was used as a marker for fragment size. The electrophoresis was done at a current of 80 W for 15-20 min in 1X TAE buffer. The gels were documented under UV light and bands were cut out using a scalpel. Fragments were purified by gel extraction (2.2.1.4).

2.2.1.2 Concentration measurements of DNA solutions

The concentration of DNA fragments or plasmids (2.2.1.4, 2.2.1.6) in 1 µl ddH_2O was measured using a spectrophotometer.

2.2.1.3 Enzyme digestion

DNA fragments and plasmids (2.2.1.4, 2.2.1.6) were cleaved by restriction enzymes. NEBuffers (with 0.1 % BSA if required) or CutSmart® Buffer were used depending on the enzyme(s). Plasmids were digested in two steps. The FavorPrep™ Kit PCR clean-up method was used to purify the product after the first digestion. Alkaline Phosphatase (CIP) was added to avoid religation of linearized plasmid DNA during the second digestion step. Digestion mixtures were incubated at 37 °C. Table 2 shows the components for digestion of plasmids and fragments. Digestion products are solutions containing mixed fragment populations which were separated by gel electrophoresis (2.2.1.1).

Table 2: Components and incubation time for plasmid and DNA fragment digestion

plasmid 1. digestion			**DNA fragment double digestion**		
buffer	1X	30 min	buffer	1X	1 h
DNA	~ 5000 ng		DNA	~ 500 ng	
enzyme 1	10 U		enzyme 1	10 U	
ddH_20 to 50 µl			enzyme 2	10 U	
			ddH_20 to 50 µl		

2. digestion		
buffer	1X	30 min
clean-up product	~39 µl	
enzyme 2	10 U	
CIP	5 U	
ddH_20 to 50 µl		

2.2.1.4 Gel extraction

Fragments were isolated by gel electrophoresis (2.2.1.1) and cut out with a scalpel. For DNA extraction the FavorPrep™ Gel/PCR Purification Kit was used following manufacturer's instructions. DNA was eluted in ddH_2O.

2.2.1.5 Isolation of genomic yeast DNA

The genome of yeast cells was extracted f. e. to verify transformations by polymerase chain reaction (PCR). 1 ml cells from an overnight culture grown in YEPB or selective medium was transferred into a microfuge tube, spun down and re-suspended in 200 µl yeast lysis buffer. 200 µl 1:1 phenol/chloroform mixture and approximately 50 µl of acid-washed glass beads were used to extract DNA. The sample was vigorously mixed for 5 min. The lysate was then centrifuged at 13,000 rpm for 5 min. The supernatant was transferred to a new tube and another 200 µl 1:1 phenol/chloroform mixture was added. The sample was again vigorous mixed for 5 min and centrifuged at 13,000 rpm for 5 minutes. In a new tube, the aqueous phase was mixed with the 0.1-fold 3M NaAc (pH 5.2) and the 2-fold 100 % ethanol and incubated for 20 min at -20 °C. The mixture was centrifuged at 13,000 rpm for 10 min. The aqueous phase was transferred into a new tube and DNA ethanol-precipitated using 2-fold of the volume 70 % ethanol. The sample was air-dried and resuspended in 20 µl ddH_2O. Genomic DNA was stored at -20 °C.

2.2.1.6 Isolation of plasmid DNA

Plasmids expressed by *E.coli* (2.2.2.3) were extracted using the Mini Plus Plasmid DNA Extraction System following manufacturer's instructions. ddH_2O was used to elute DNA. Plasmids were stored at -20 °C.

2.2.1.7 Ligation

After enzyme digestion (2.2.1.3), DNA fragments can be inserted into a vector by the creation of recombinant DNA molecules. For ligation 1X T4 DNA ligase buffer, 200 U T4 Ligase, insert and vector (weight ratio 3:1) were mixed and filled up to 10 µl with ddH_20. The ligation mix was incubated at 25 °C for 1 h and directly used for transformation (2.2.2.3).

2.2.1.8 PCR using Taq DNA Polymerase

PCR is a common method to selectively amplify DNA fragments by primers and a thermostable DNA polymerase. The two primers contain complementary sequences to the target region of the DNA template. To verify transformations of *E. coli* or yeast cells (2.2.2.3, 2.2.2.9), DNA was amplified using a thermocycler with a sample size of 25 µl in PCR tubes. The components where mixed as followed:

Table 3: Components of a PCR using Taq DNA Polymerase

component	volume (µl)	final concentration
buffer (10x)	2.5	1x
dNTP (2.5 mM)	1	100 µM
forward primer (10 µM)	1	0.5 µM
reverse primer (10 µM)	1	0.5 µM
Taq DNA Polymerase (250 U)	0.125	1.25 U/µl
ddH_20	19.375	

For *E. coli* colony PCR, cells were transferred directly into the tubes using a sterile toothpick. Primers binding to the vector and the insert were chosen to ensure that the fragment is inserted correctly into the vector (2.2.1.7). In yeast colony PCR, 1 µl of the

ddH_2O was replaced by 1 µl of lysis solution (2.2.1.10). Unless otherwise indicated, the annealing has taken place at a temperature of 50 °C. The thermocycling conditions were chosen as followed:

95 °C	5 min	1 cycle
95 °C	30 sec	30 cycles
50 °C	1 min	
72 °C	~ 1 min/kb	
72 °C	10 min	1 cycle
4 °C	∞	

2.2.1.9 PCR using Q5 High-Fidelity DNA Polymerase

PCR was also used to amplify DNA fragments for enzyme digestion (2.2.1.3). To avoid unintended mutations during amplification, Q5 Polymerase was utilized. This DNA polymerase supports a robust DNA amplification with an error rate ~280-fold lower than that of Taq DNA Polymerase. The composition of a reaction is shown in Table 4.

Table 4: Components of a PCR using Q5® High-Fidelity DNA Polymerase

component	volume (µl)	final concentration
Q5® Reaction Buffer (5x)	5	1x
Q5® High GC Enhancer (5x)	5	1x
dNTP (2.5 mM)	1	100 µM
forward primer (10 µM)	1.25	0.5 µM
reverse primer (10 µM)	1.25	0.5 µM
template DNA		~ 100 ng
Q5® High-Fidelity DNA Polymerase	0.250	0.02 U/µl
ddH_20	to 25	

The annealing temperature (T_a) of the primers depends on the length of the complementary sequence and the percentage of G and C. The online tool NEB T_m Calculator* was used to determine the melting temperature (T_m) of the primers and find the optimal T_a for different primer pairs. Typically the T_m can be found within a range of 50 °C to 72 °C. The cycling was preceded as followed

*http://tmcalculator.neb.com/#!/

98 °C	30 min		1 cycle
98 °C	10 sec	}	35 cycles
50 - 72°C	30 sec		
72 °C	~ 30 sec/kb		
72 °C	2 min		1 cycle
4 °C	∞		

2.2.1.10 Cell lysis for yeast colony PCR

Due to their cell wall yeast cells needed to be lysed before PCR. Cells were picked from a colony and transferred into a PCR tube containing 20 µl NaOH (0.1 M). The samples were incubated for 10 min at 95 °C and then centrifuged for 10 min at maximum speed. 1 µl supernatant can be used in 25 µl reaction size for PCR.

2.2.2 Microbiological methods

2.2.2.1 Cell cycle arrest

To activate the SAC, yeast cells were arrested in G_2 phase using benomyl. Cells were grown in overnight cultures at 25 °C, diluted and grown again to early log phase (OD_{660} ~ 0.3). 1 ml YEPD medium was transferred into a tube and heated at 95 °C. 1 µl of benomyl stock were added to the medium and mixed well. It was heated again to minimize benomyl precipitation, then slowly cooled down at room temperature. 1 ml of yeast culture in early log phase was spun down for 2 min at 4000 rpm. Cells were re-suspend in a benomyl-containing medium. The culture was incubated at 25 °C for 90 to 120 min. Cells were imaged directly or fixed with methanol (2.2.2.8).

2.2.2.2 Cell density measurement of yeast cultures

The optical density (OD) of liquid yeast cultures were measured at a wavelength of 660 nm using a photometer.

2.2.2.3 Transformation of competent *E. coli* cells

E.coli cells were used for high-level plasmid production. Therefore up to 5 µl of ligation product (2.2.1.7) or 500 ng plasmid were added to 50 µl competent *E.coli* cells (CMK603). The sample was incubated for 20 min on ice and then heat-shocked at 37°C for 1 min. 500 µl 2XTY buffer was added, and the cells were incubated for 35 min at 37 °C. Cells were harvested by centrifugation for 5 min at 3000 rpm. The extra medium was removed and 100 µl were left to re-suspend the pellet. The mixture was then spread on LB agar plates containing 100 µg/µl ampicillin and incubated at 37°C overnight. Transformations with ligation product were verified by PCR (2.2.1.8), single plasmid-containing colonies were used to set up liquid cultures (2.2.2.4)

2.2.2.4 Cultivation of plasmid-containing *E.coli* cultures

For plasmid production, LB medium containing 100 µg/µl ampicillin was inoculated by single transformed *E.coli* colonies grown on LB agar plates (2.2.2.3). Liquid cultures were shaken at 220 rpm at 37 °C for 12 to 16 h. Plasmids were extracted using the FavorPrep™ Gel/PCR Purification Kit (2.2.1.6).

2.2.2.5 Cultivation of yeast strains

For long-time storage, strains were frozen at -80 °C in glycerol. The cells were directly transferred into a glycerol filled tube. Frequently used strains were patched on plates containing YEPD or selective medium and incubated at 25 °C or 30 °C for 2-3 days and then stored at 4 °C. The patches were used to inoculate media for liquid cultures. Cultures were grown overnight at 25 °C or 30 °C and diluted at the next morning.

2.2.2.6 DAPI-staining of the nucleus

Ethanol treatment makes the yeast cell wall permeable to DAPI. Therefore ethanol stored cells were used for staining. Cells were washed in ddH_2O or PBS and re-suspend in 2.5 µg/ml DAPI solution in H_2O. The samples were imaged directly under the microscope (2.2.4.2).

2.2.2.7 DMSO-enhanced whole cell yeast transformation

DMSO transformations were used to transform plasmids into yeast cells. Cells were grown at 25 °C in overnight cultures, diluted and grown to mid-log phase (OD_{660} ~ 0.5) in YEPD or selective media. 1 ml of cells were harvested by centrifugation at 4000 rpm for 2 min. Then the cells were washed with 100 µl LiOAc/TE 8.0 and resuspended in 100 µl LiOAc/TE 8.0. Samples were gently shaken by hand, and ~ 500 ng plasmid was added. After gently mixing, the cells were incubated for 5 min at room temperature. 280 µl 50 % PEG 4000 were added, mixed by inverting 4-6 times and then incubated again for 45 min at 30 °C or 1 h at 25 °C. 43 µl DMSO was added, and the sample was heat-shocked for 5 min at 42 °C. After centrifugation for 30 sec at 12000 g, the cells were washed in ddH_2O, re-suspended in 100 µl ddH_2O and then spread onto two plates containing selective media. Plates were incubated at 25 °C. Transformations were verified by PCR after 2-3 days (2.2.1.8).

2.2.2.8 Fixation of yeast cells

Before imaging, most of the yeast cell samples were fixed. Cells were harvested by centrifugation for 2 min at 4000 rpm and then washed with ddH_2O or PBS buffer. The pellet was re-suspend in ice-cold methanol and incubated for 20 min at -20 °C. Then the sample was spun down and washed with ddH_2O or PBS. Cells were stored at -20 °C in 70 % ethanol. Before imaging, the nucleus was stained using 4',6-diamidino-2-phenylindole (DAPI) (2.2.2.6).

2.2.2.9 High-efficiency yeast transformation

DNA fragments were integrated into yeast genome using high-efficiency yeast transformation. Cells were grown at 25 °C in overnight cultures, diluted and grown to mid-log phase (OD_{660} 0.4 ~ 0.6) in YEPD media. Cells were harvested by centrifugation at 3000 rpm for 2 min and washed in 200 µl ddH2O. After centrifugation, the pellet was

re-suspended in 60 µl 100 mM LiOAc and incubated at 30 °C for 15 min. The samples were spun down at 3000 rpm for 2 min and

PEG 3350 (50 %)	48 µl
LiOAc (1 M)	7.2 µl
ssDNA (2 mg/ml)	10 µl
DNA	~ 500 ng
ddH_2O	to 73 µl

were added. Single-stranded DNA (ssDNA) was heated at 95 °C for 5 min before use. The mixture was incubated at 30 °C and 42 °C for 30 min each. Cells were washed with ddH_2O, resuspended in 100 µl ddH_2O and spread onto two plates containing selective media. Plates were incubated at 25 °C. Transformations were verified by PCR after 2-3 days (2.2.1.8).

2.2.2.9 Serial dilution of yeast cells

Serial dilution was used to compare the vitality of transformed yeast cells. Strains were grown at 25 °C in overnight cultures, diluted and grown to mid-log phase in YEPD or selective media. Cell densities were measured (2.2.2.2). 10^7 cells of each sample were centrifuged and re-suspended in 50 µl ddH_2O to normalize the cell number. Ten-fold dilutions of cell suspensions were prepared and 5 µl each were spotted onto plates containing YEPD or selective media. Plates were incubated at 25 °C or 37 °C. Results were documented by photographing after 24 and 48 h.

2.2.3 Protein chemical Methods

2.2.3.1 Isolation of whole-cell protein

To detect proteins using western blot, the whole-cell protein was isolated from yeast cells. Cells were grown at 25 °C in overnight cultures, diluted and grown to mid-log phase in YEPD or selective media. The Cell densities were measured as described above (2.2.2.2). 10^7 cells were harvested by centrifugation for 1 min at maximum speed, and the pellet was

resuspended in 200 µl 0.1 M NaOH. The sample was incubated for 5 min at room temperature and spun down again. The pellet was resuspended in

Sample buffer (SB) (2x)	98 µl
Protease inhibitor (PI) (100x)	1 µl
Pefabloc® SC (200 mM)	0.5 µl
Dithiothreitol (DTT) (1 M)	0.5 µl

and incubated for 5 min at 95 °C. Then the mixture was centrifuged at maximum speed for 1 min, and the supernatant was used for SDS-PAGE or stored at -20 °C.

2.2.3.2 Sodium dodecyl sulfate-polyacrylamide gel electrophoresis (SDS-PAGE)

SDS-gels containing 15 % separation and 5.6 % stacking gel (Table 5) were inserted into the electrophoresis chamber. Stored whole-cell protein isolates (2.2.3.1) were cooked for 5 min at 95 °C and centrifuged at maximum speed for 1 min. The supernatant was used to fill the wells of the stacking gel. A protein ladder was used as a marker for protein size. Running buffer was added, and the electrophoresis was done at a current of 60 mA for ~ 2 hours. After, proteins were transferred from the gel into a membrane.

Table 5: Components of separating (left) and stacking (right) gels for SDS-PAGE

separating gel (15 %)	**volume (ml)**	**stacking gel (5.6 %)**	**volume (µl)**
acrylamide mix	7.5	acrylamide mix	800
Tris buffer (1.5 M, pH 8.8)	3.75	Tris buffer (1 M, pH 6.8)	625
SDS (10%)	0.15	SDS (10%)	50
ddH_2O	3.5	ddH_2O	3,500
APS (10 %)	0.15	APS (10 %)	50
TEMED	0.015	TEMED	5

2.2.3.3 Western blot analysis

Western blot method was used to detect membrane-bound proteins. The Proteins were separated by size using SDS-PAGE (2.2.3.2) and transferred to a membrane using a transfer tank and transfer buffer overnight at a current of 200 mA. The membrane was

stained with Ponceau S and washed on an orbital shaker in PBST buffer afterward. Blocking solution was used to saturate the membrane with proteins for 1 hour. The membrane was incubated with the primary antibody, diluted in blocking solution for 1 hour. Antibodies and dilutions can be found in Table 6. Unbound antibodies were washed away during a 3 times washing step for 10 min each using PBST. The membrane was incubated for 30 min with the diluted secondary antibody, and washed again 3 times. Protein bands were detected using the enhanced chemiluminescence method (ECL). Detection reagent 1 and 2 were mixed in equal shares and given onto the membrane. The x-ray film was exposed to chemiluminescence in a dark chamber for up to 10 min.

Table 6: Dilutions of primary and secondary antibodies in blocking buffer

primary antibody	dilution (v/v)	secondary antibody	dilution (v/v)
anti-GFP	1:1000	anti-mouse	1:3000
anti-Mad 2	1:200	anti-rabbit	1:3000
anti-Bet1	1:2000		

2.2.4 Microscopy

2.2.4.1 Concanavalin A coating of microscope slides

Multiwell microscope slides were coated with concanavalin A (ConA) to avoid cell movement during imaging. 15-20 µl of 1 mg/ml ConA in ddH_2O was filled into each well. After 5 min the solution was removed, and the slide was covert and air-dried for some hours. The wells were washed with ddH_2O and dried again. Slides can be stored for about 1 week at room temperature.

2.2.4.2 Imaging and processing

Yeast cells grown to mid-log phase or fixated cells (2.2.2.8) were harvested by centrifugation and washed once with ddH_2O, then re-suspended in ddH_2O. 1 µl cells suspension was placed into the wells of ConA coated multiwell slides and examined immediately. A wide-field epifluorescence microscope was used to image the cells.

Exposure times of 1 s for DAPI and 5 s for EmCitrine were used. For DIC images the exposure time was calculated automatically. The software SPOT Advanced was used to regulate the settings. Digital images were processed with ImageJ.

3 Results

3.1 Plasmid design and creation of *mad2*△ + *MAD2 – EmCit* strain

A plasmid called 413-MAD2-EmCit was utilized to generate the plasmid 413-MAD2-EmCit-LEU2 used in this study (Figure 5). 413-MAD2-EmCit contains a *MAD2* gene linked at its C-terminus via a flexible Gly-Ala (2x) (GAGA) linker to the N-terminus of *EmCitrine* (*EmCit*) inserted into the multiple cloning site of a pRS413 plasmid. The introduced construct is under the control of the *MAD2* native promoter. pRS413 is a yeast centromere plasmid (YCp) and therefore considered as low copy vector. It incorporates a part of an autonomously replicating sequence (ARS) containing yeast origin of replication and a segment of a centromere sequence (CEN) (Marczynski and Jaehning, 1985). Furthermore, the vector carries the *bla* (AmpR) marker allowing selection with ampicillin during replication in *E. coli*. *HIS3* is an auxotrophic yeast marker for L-histidine synthesis. YCps are typically found as a single copy per cell and replicate as if they are small independent chromosomes. Nevertheless, checkpoint activity is sensitive to over or underexpression of Mad2 wherefore the *MAD2-EmCit* construct should be integrated into yeast genome by homologous recombination (Mariani et al., 2012).

I inserted the auxotrophic selection marker *KILEU2* flanked with a Cre-Lox recombination (2x loxP) into 413-MAD2-EmCit. Cleavage of plasmid and insert was performed by the restriction enzymes NotI and SacII around 200 bp downstream of *EmCit* stop codon (Figure 5). The correct placement of *loxP-KILEU2-loxP* was verified by PCR using two primers flanking the insert (Figure 6a). The selectable marker will laster be integrated along with the construct into yeast genome to indicate the success of the transformation. *KILEU2* provides leucine prototrophy to cells expressing Mad2-EmCit. After a successful integration of the *MAD2-EmCit-KILEU2* fragment into yeast, *KILEU2* can be cleaved and reused as a selection marker for further transformations in the same

strain. *KILEU2* loxP sites are going into the same direction. Therefore, expression of the enzyme Cre recombinase after transformation with the appropriate plasmid results in deletion of *KILEU2*.

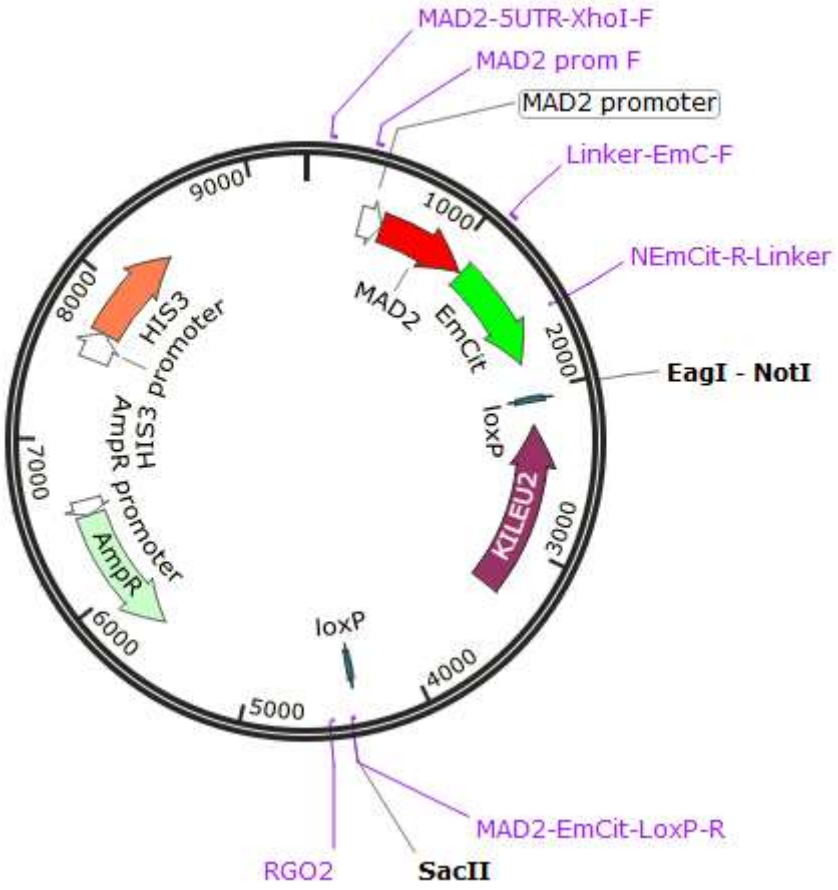

Figure 5: Transcription map of 413-MAD2-EmCit-LEU2. The pRS413 plasmid contains *MAD2* (red) with its native promoter (white) and *EmCitrine* (green), linked with a GAGA sequence (not shown). *KILEU2-Loxp* (violet, blue) was inserted utilizing NotI (position 2019) and SacII (position 4414) as restriction sites. Primers are shown in violet at their binding sites. Binding sites at the outer DNA strain of the plasmid indicate forward primers, at the inner strain reverse primers.

413-MAD2-EmCit-LEU2 was transformed into *E.coli* for replication. The primers MAD2-promoter-F and MAD2-EmCit-LoxP-R, shown in Figure 5, were used to amplify the *MAD2-EmCit-KILEU2* fragment by PCR from 413-MAD2-EmCit-LEU2 for yeast transformation. The *MAD2* promoter sequence and a sequence at the 3´ end of the fragment, generated by MAD2-EmCit-LoxP-R primer, were used as homologous sequences for homologous recombination. I integrated the DNA into the genome of a *MAD2* deletion strain (*mad2*∆) to verify the correct placement of the fragment. In *mad2*∆, the selection marker *KanMX4,* which acquires resistance to geneticin (G418), replaces *MAD2*. However, the *MAD2* promoter retaines upstream. Figure 6b depicts the situation in *mad2*∆ (lower outline) and shows the expected place of fragment integration into the strain (upper outline). Crosses symbolizes homologous recombination. Successful integration of *MAD2-EmCit-KILEU2* is shown in the Figures 6c and d. Figure 6c shows that the colonies 1 to 4 are not able to grow on a geneticin-containing plate. Instead, they can grow on a plate leaking leucine (-LEU), whereas *mad2*∆ shows geneticin resistance, but no leucine prototrophy. The replacement of *KanMX4* by *KILEU2* in all four colonies leads to the assumption that *MAD2-EmCit-KILEU2* was inserted at its intended place. Besides, the integration was verified by PCR using a primer (MAD2-5UTR-XhoI-F) which can bind to plasmid and chromosome, but not to the fragment (Figure 6d).

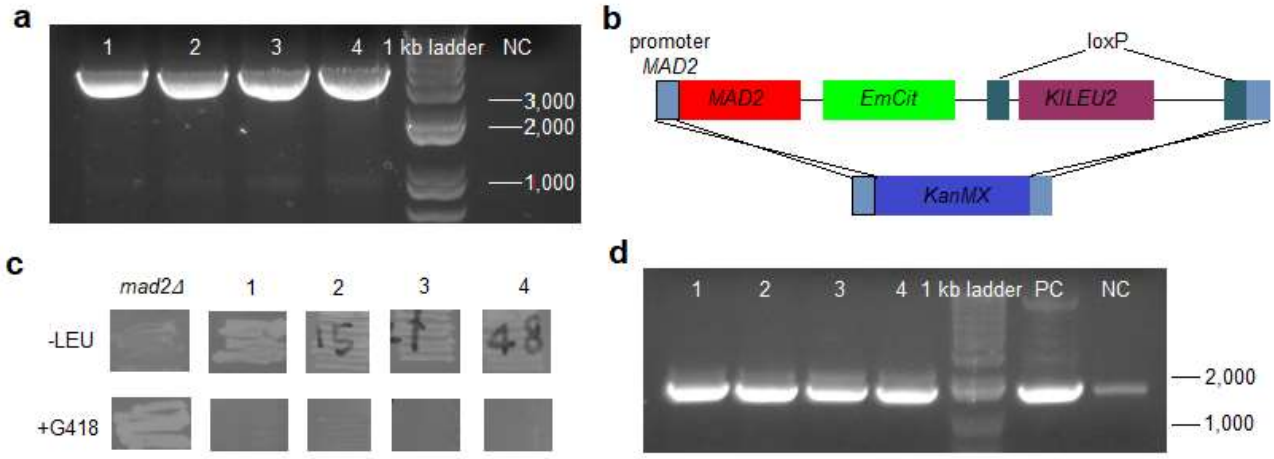

Figure 6: Transformation of *mad2*Δ. (a) Gel electrophoresis of *E.coli* colonies. Colony 1-4 transformed with MAD2-EmCit-LEU2-413 ligation mix show a band of the correct size. Linker-EmC-F and RGO2 were used as primers to amplify the fragment of around 3,200 bp. A DNA-free PCR mix was used as negative control (NC). (b) The construct amplified from MAD2-EmCit-LEU2-413 was transformed into a *mad2*Δ strain using homologous recombination. MAD2-promoter-F and MAD2-EmCit-LoxP-R were used as primers. (c) A growth test on -LEU and +G418 plates shows the replacement of *KanMX4* by the *KILEU2* containing construct in 4 colonies of *mad2*Δ. (d) Verification of the transformation by PCR using the primers MAD2-5UTR-XhoI-F and NEmCit-R-Linker. The fragments size was around 1,400 bp, and the plasmid MAD2-EmCit-LEU2-413 was used as positive control (PC).

Figure 7a shows that the fluorescence signal of EmCit could be detected in microscopic studies of the colonies. The expected localization of Mad2-EmCit in cycling cells is the nuclear envelope, where Mad2 is associated with the nuclear pore complexes (NPCs) (Iouk et al., 2002). To verify co-localization with Mad2-EmCit, I stained the nucleus of microscopic examined cells using 4',6-diamidino-2-phenylindole (DAPI). Since DAPI and EmCit are coincident, I assumed the localization of the fusion protein at the NPCs of the cells. Figure 7b shows an immunoblot to detect Mad2-EmCit by anti-GFP antibodies in protein extracts of *mad2*Δ*+MAD2-EmCit*. The extracts of transformants 1-4 were electrophoretic separated by polyacrylamide gel and stained with anti-GFP antibody. All

four transformants show a band between 37 and 49 kDa, larger than single EmCit (27 kDa) or Mad2 (22 kDa), which can be assumed to be the fusion protein. Apart from the specific Mad2-EmCit band, the blot shows unspecific bands in the range of unbound EmCit or Mad2, which also appear in negative controls.

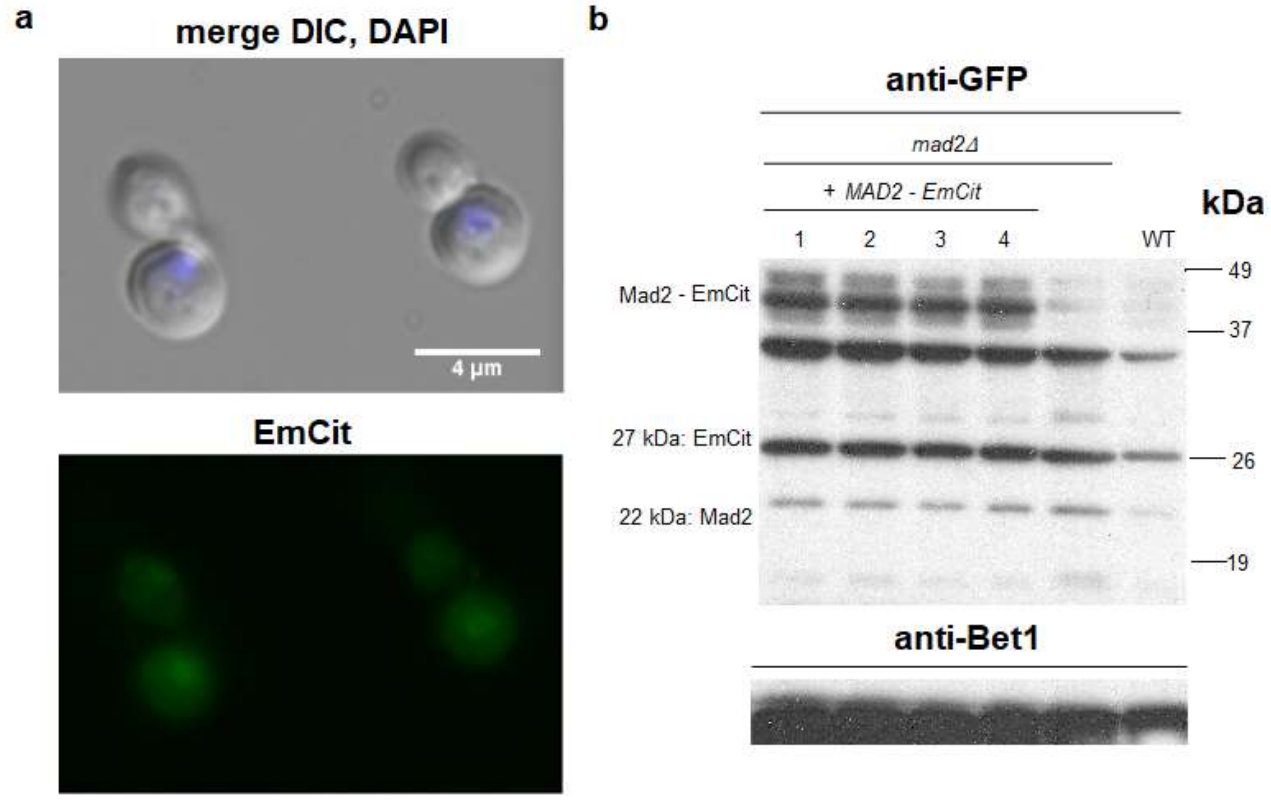

Figure 7: Detection of Mad2-EmCit by microscopy and anti-GFP antibodies. (a) DIC image of cells with a DAPI-stained nucleus in blue (top). Excitation of EmCit leads to clear fluorescence signal in the area of the nucleus (below). Cells were grown to log phase at 25 °C, fixated and stained. (b) Detection of the fusion protein by immunoblotting. Protein extracts were prepared from cells in log phase and analyzed by immunoblotting using indicated antibodies. The fusion protein could be detected in all four transformants. Bands in the range of unbound EmCit or Mad2 are unspecific since they also appear in *mad2*Δ and BY4741 (wild type, WT) strains. Bet1 serves as loading control.

3.2 SAC activation by benomyl

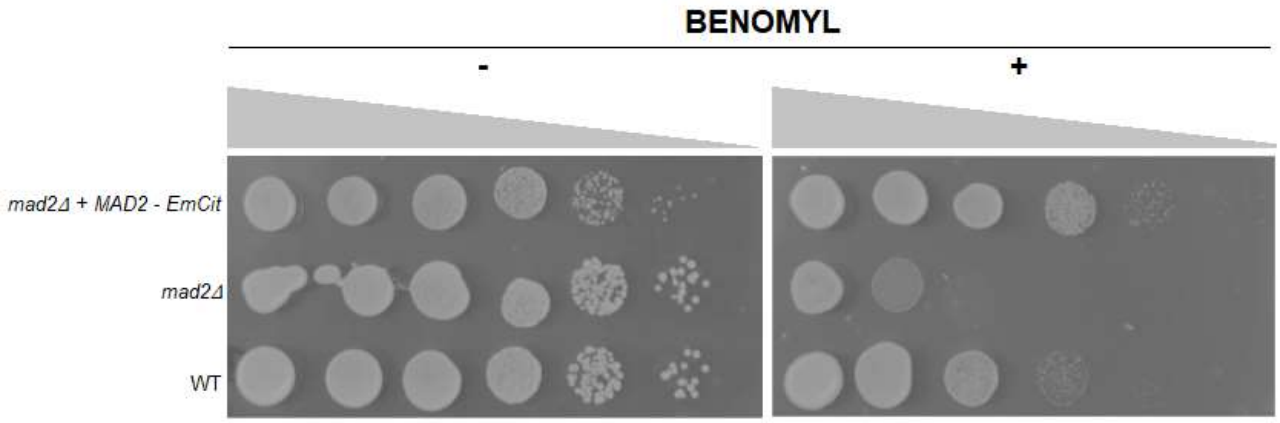

Figure 8: Benomyl sensitivity of *mad2*Δ + *MAD2-EmCit* strain. Cells were spotted on YEPD plates with or without 30 µg/ml benomyl in 10-fold dilutions starting from 10^6 to 10^1 cells per spot. Plates were incubated at 25 °C for 48 h. Benomyl binds to microtubules, inhibits their polymerization and binding ability to the kinetochores. *mad2*Δ leaks Mad2 and cannot activate the SAC to delay G_2 phase which leads to growth defects. Mad2-EmCit can restore the WT and react less sensible to the drug.

During G_2 phase of the cell cycle, the kinetochores of sister chromatids need to be attached by microtubules in order to be equally distributed between mother cell and bud. The drug benomyl binds to microtubules and inhibits their polymerization, which leads to unattached kinetochores. In response, SAC activation prolongs G_2/M phase transition until all kinetochores are connected to the spindle apparatus. Mad2 recruitment to unattached kinetochores is an early step of checkpoint activation. Along with other subunits, Mad2 binds Cdc20 to form the mitotic checkpoint complex. A strain leaking Mad2 (like *mad2*Δ) cannot activate the checkpoint. The result is unequal chromosome distribution and increased benomyl sensitivity. Figure 8 shows the increased benomyl sensitivity of *mad2*Δ as a result of the *MAD2* deletion. Strains were spotted on plates with and without benomyl. A spot of the *mad2*Δ strain containing 10^4 cells cannot grow any visible colonies, whereas the WT spawns single colonies out of 10^3 cells. However, *mad2*Δ + *MAD2-EmCit* shows even a stronger growths than the WT on a drug-containing plate. Since *MAD2-EmCit* can

rescue the *mad2*Δ strain, I assume that the fusion protein can activate the SAC. The fluorescence signal of Mad2-EmCit (Figure 7a) and the result of the growth test suggest a functional fusion protein.

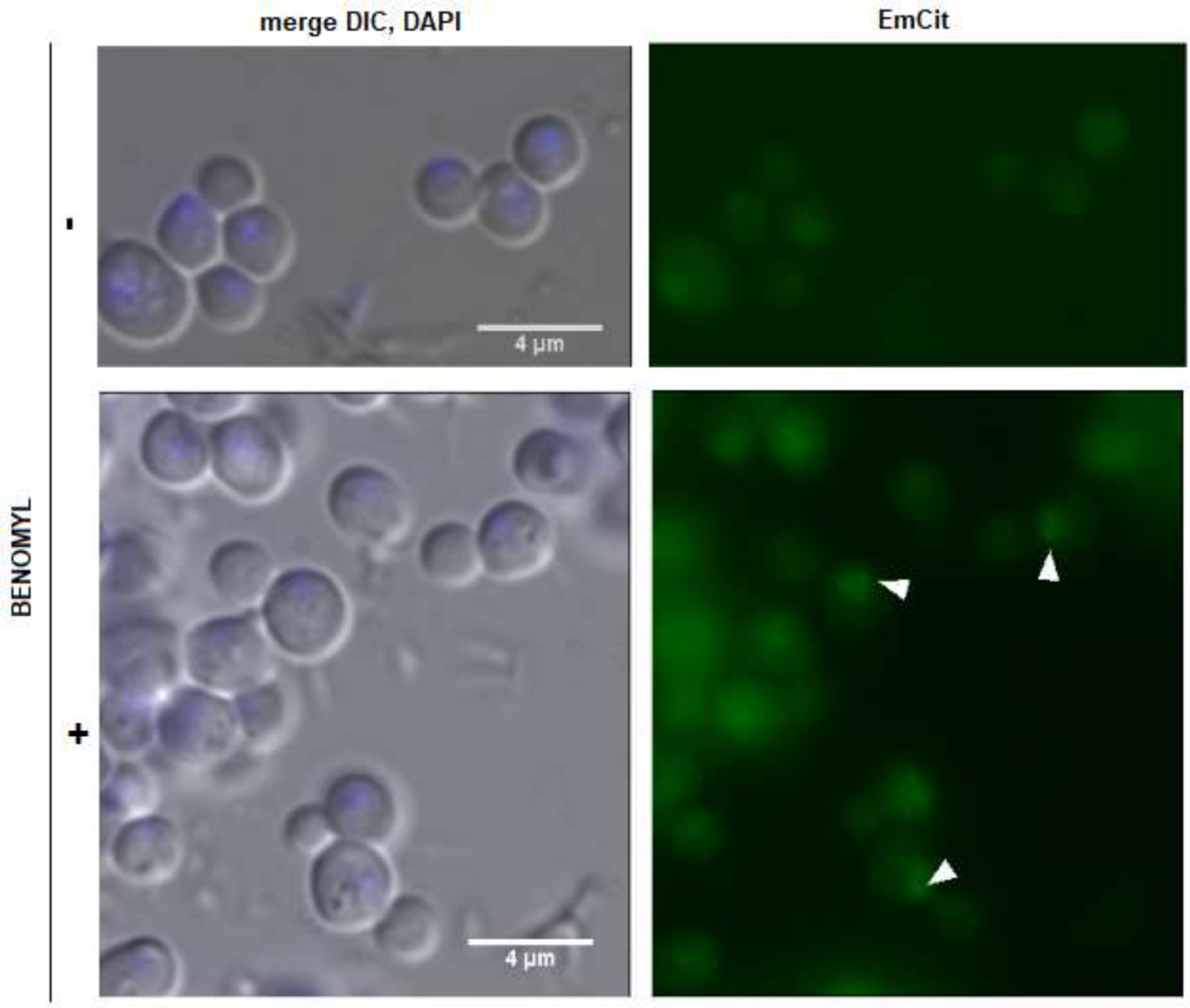

Figure 9: Fluorescence microscopy images of benomyl-treated and untreated cells. DIC images with DAPI stained nucleus in blue (left), Mad2-EmCit in green (right). Cells were grown to early log phase and then transferred either to YEPD or medium containing 30 µg/ml benomyl. Strains were grown at 25 °C for 120 min, fixated, stained and examined by microscopy. EmCit image shows a weak background fluorescence and a stronger signal in the area of the nucleus (top). Some benomyl-treated cells are in G_2/M phase (left) and show brighter fluorescence (arrows) in the nucleus area (below).

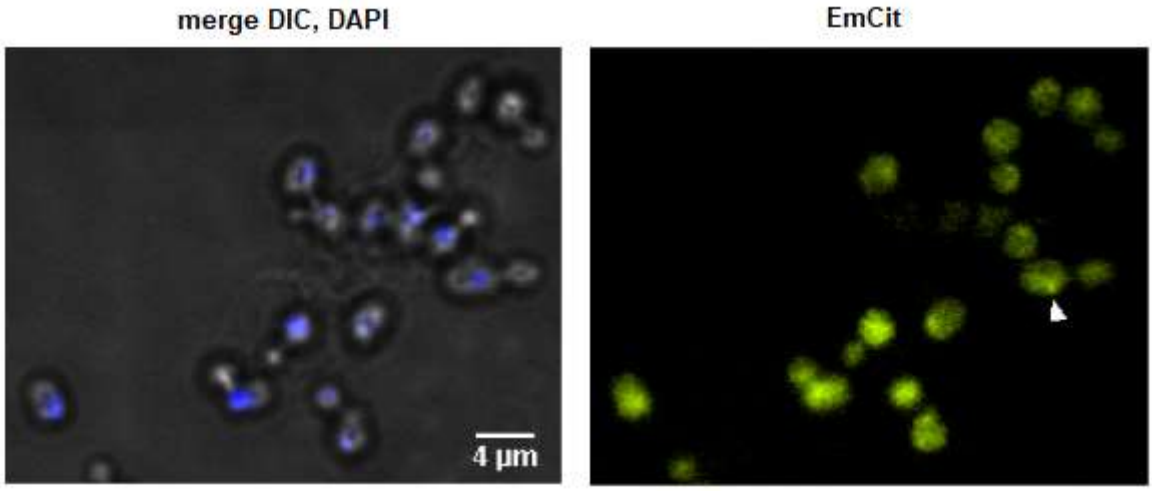

Figure 10: Fluorescence microscopy images of benomyl-treated cells using a piezo stage. Cells were prepared as described in Figure 9. An arrow marks a stronger EmCit signal (right).

To test, if the fusion protein is appropriate to visualize checkpoint activation, a location shift of Mad2-EmCit needs to be observable. The fluorescence signal of tagged Mad2 should shift from nuclear envelope (SAC OFF) to kinetochore foci in case of an activated checkpoint. Therefore *mad2*Δ + *MAD2-EmCit* liquid cultures were incubated in YEPD medium containing benomyl. The drug should arrest most of the cells in G_2/M phase by activating the mitotic checkpoint. Arrested cells should have grown a large bud, and their single nucleus should be located in the mother cell close to the bud neck. In order to arrest the cells, I tested benomyl, nocodazole and a mix of both, different drug concentrations, incubation times and methods. Using benomyl leads to the best results. The cells were stained using DAPI to visualize nucleus number and position. Nevertheless, *mad2*Δ + *MAD2-EmCit* neither show a high percentage of arrested cells nor clear kinetochore foci (Figure 9). Although benomyl seemed to arrest some cells in G_2/M phase, a Mad2-EmCit location shift was not visible. Figure 9 depicts microscopic images of examined cells. A few relatively bright spots located in the outer region of the nucleus, are marked with white arrows

In arrested cells, the signal of kinetochore-bound Mad2-EmCit could be too weak to be detectable using manual focus. A piezo stage to control the z-axis position of the objective was used to image different slices of the cell (Figure 10). A white arrow shows a brighter spot. But also this microscopy method fails to detect a kinetochore signal. It remains unclear, whether Mad2-EmCit is not fully functional or benomyl is not able to destabilize the microtubules of the strain.

3.3 Transformation of *vps74-1/mad2*Δ

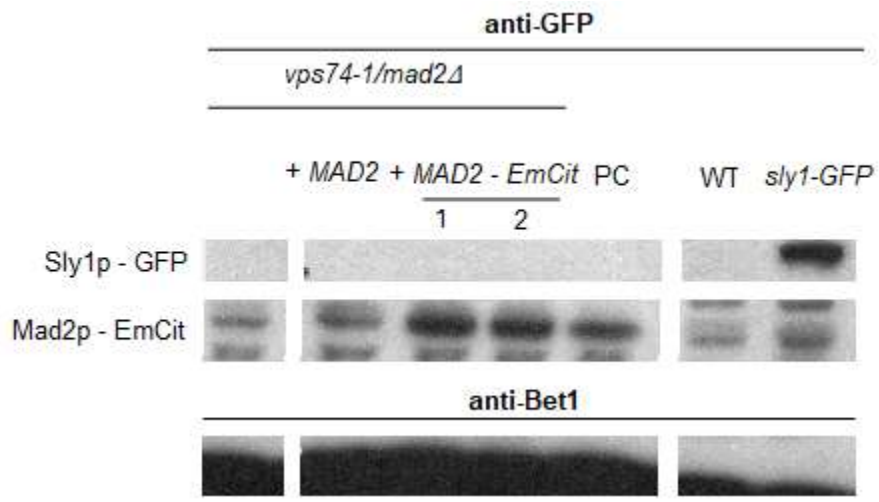

Figure 11: Verification of *vps74-1/mad2Δ* + *MAD2-EmCit.* Immunoblot of *vps74-1/mad2Δ* transformed either with *MAD2* or *MAD2-EmCit.* Mad2-EmCit was detected in *vps74-1/mad2Δ* + *MAD2-EmCit* and PC (*mad2Δ* + *MAD2-EmCit*). *sly1-GFP* was used as antibody binding control. *vps74-1/mad2Δ, vps74-1/mad2Δ* + *MAD2,* WT and *sly1-GFP* show an unspecific band. *Bet1* was used as loading control.

vps74-1 is a *vps74*$^{R6\text{-}8A}$ mutant with a *ted1Δ* background. The vacuolar protein sorting-associated protein 74 (Vps74) mediates the adherence of a Golgi glycosyltransferases subset, and the protein Ted1 acts in cargo exit from endoplasmic

reticulum together with Emp24/Erv25 (Haass et al., 2007). *vps74-1* is temperature sensitive (Ts), though deletion of certain genes can rescue the strain. Those genes encode proteins required for SAC activation like *MAD1* and subunits of MCC (*MAD2, MAD3, BUB3*). Therefore it is assumed, that the Ts phenotype in *vps74-1* appears as a result of SAC activity. In addition, the strain is sensitive to calcofluor white (CW), a drug binding to cell wall chitin. *vps74-1/mad2Δ* is a *MAD2* deletion mutant of *vps74-1*.

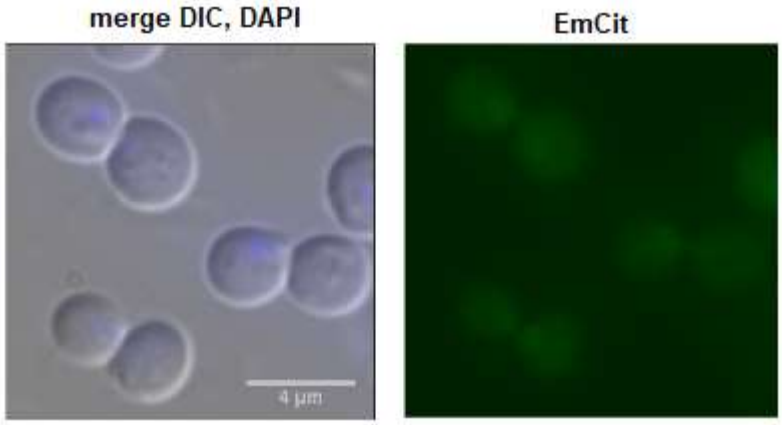

Figure 12: Microscopic images of *vps74-1/mad2Δ + MAD2-EmCit*. Cells were grown to early log phase at 25 °C, fixated, stained and examined by microscopy. EmCit signal (green) is observable in the area of the nucleus (blue).

The *MAD2-EmCit* fragment was transformed into *vps74-1/mad2Δ* to test, whether Mad2-EmCit can restore the phenotype of *vps74-1*. Besides, an unaltered *MAD2* gene was transformed into a different *vps74-1/mad2Δ* strain to observe any differences in growth or physiology to cells expressing Mad2-EmCit. Figure 11 shows an immunoblot of *vps74-1/mad2Δ + MAD2-EmCit.* Transformants were screened and picked for further growth tests. Depicted in Figure 12 are microscopic images of *MAD2-EmCit+MAD2-EmCit*. The fluorescence signal of Mad2-EmCit is located in the nucleus area.

A functional Mad2-EmCit should be able to restore the phenotype of the *vps74-1* strain. Moreover, it should be consistent with the *vps74-1 + MAD2* phenotype. The results of a growth test show the strongly increased Ts phenotype of *vps74-1/mad2Δ + MAD2-EmCit* (Figure 13). The cells are not able to grow at 37 °C, whereas cells expressing the unaltered Mad2 show a similar phenotype to *vps74-1.*

Expression of either Mad2 or Mad2-EmCit could rescue the benomyl sensitive *vps74-1/mad2Δ* strain (Figure 13a). On CW containing plates, *vps74-1/mad2Δ + MAD2-EmCit* and *vps74-1/mad2Δ + MAD2* showed a similar phenotype to *vps74-1* (Figure 13b). However, neither temperature shift to 37 °C nor benomyl treatment led to a visible location shift of Mad2-EmCit in *vps74-1/mad2Δ + MAD2-EmCit* in microscopic examined cells.

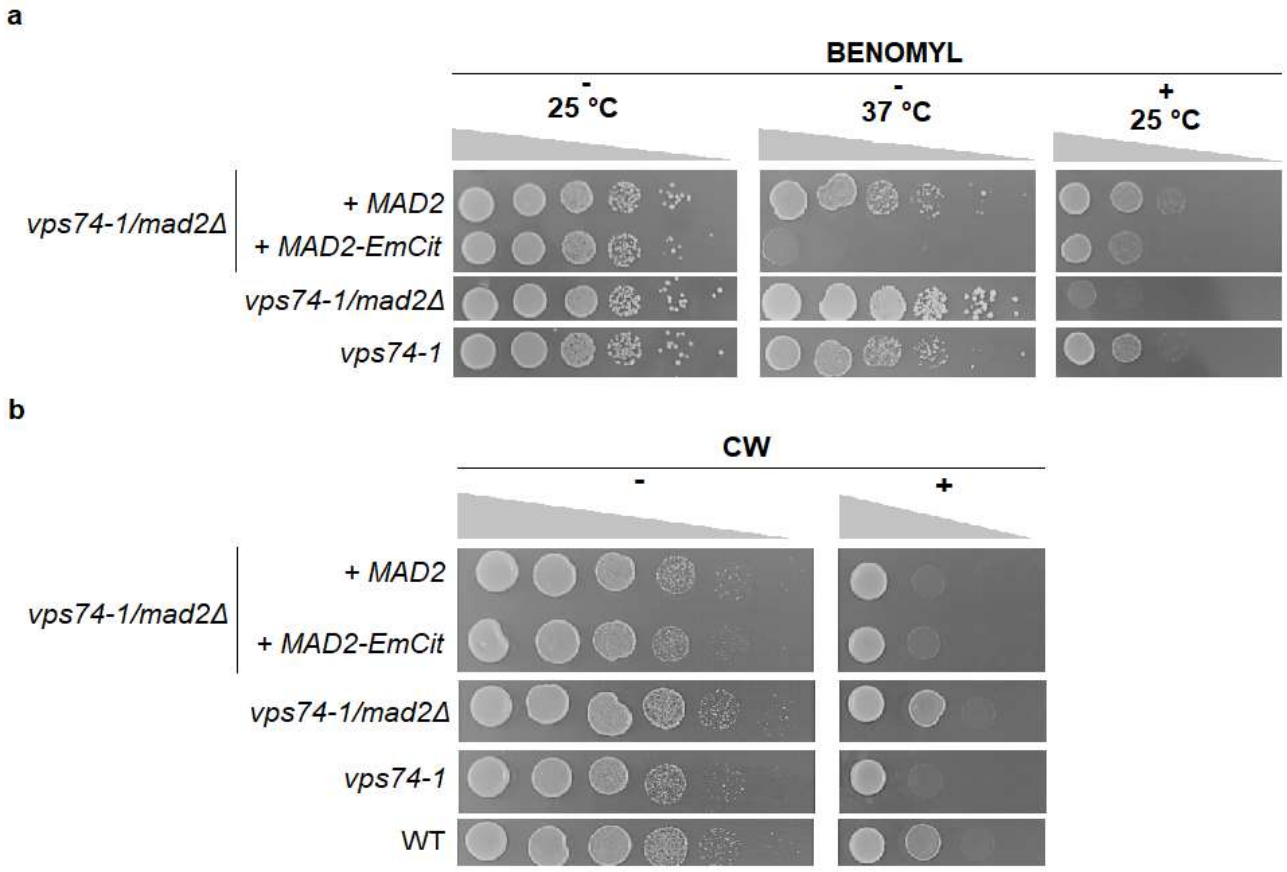

Figure 13: Serial dilution of transformed *vps74-1/mad2Δ* strain. (a) *vps74-1/mad2Δ + MAD2-EmCit* shows a strongly increased Ts phenotype, whereas *vps74-1/mad2Δ + MAD2* appears with the same phenotype as *vps74-1.* Strains were patched on YEPD plates with and without 30 µg/ml benomyl and incubated at indicated temperatures for 48 h. Benomyl sensitivity is decreased in cells expressing either Mad2 or Mad2-EmCit. (b) Strains were patched on a CW containing plate and incubated at 25 °C for 48 h. Strains expressing both kinds of Mad2 can restore the *vps74-1* phenotype.

3.4 Transformation of *vps74-1/mad2*△ with split-EmCit

One reason for an invisible location shift of tagged Mad2 could be the high background fluorescence unbound O-Mad2. Usage of split-GFPs could eliminate background fluorescence. This technique is mostly used for detection and imaging of protein-protein interactions *in vivo*. Two binding partners are labeled with two different nonfluorescent portions of GFP each. The GFP parts need to assemble to restore a fluorescent protein. By binding of the two tagged proteins, split-GFP can auto-assemble create a fluorescent protein (Xie et al.; 2017). Once assembled, split-GFP cannot dissociate.

In this study, two proteins, Mad1 and Mad2, were tagged with different nonfluorescent portions of split-EmCit each. Figure 14a shows the re-assembled fluorescent structure of the two EmCit portions. The N-terminus of Mad1 is linked to the N-terminal part of split-EmCit (NEmCit) and regulated by the endogenous Mad1 promoter. The C-terminal portion of split-EmCit (CEmCit) labels Mad2 at its N-terminus. A strong *TPI* promoter initiates transcription of the fusion protein (Figure 14b). By binding of Mad1 and Mad2 in the early stage of SAC activation, the two EmCit parts should auto-assemble and show a fluoresce signal. Indeed, the two EmCit parts do not dissociate by themselves, which should lead to a stable EmCit-Mad1-Mad2 complex.

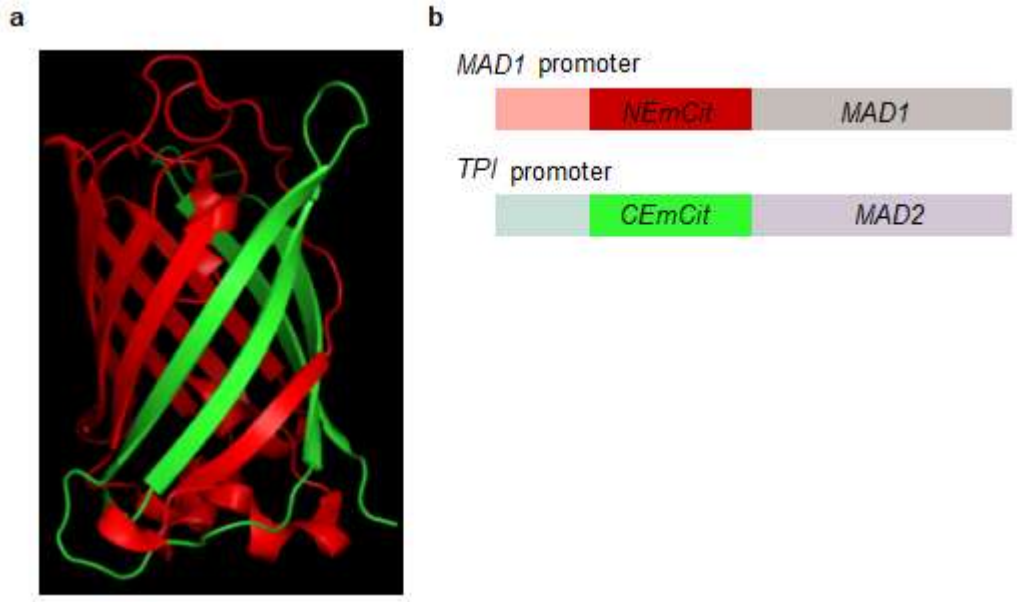

Figure 14: Split-EmCit and tagged Mad1/2. (a) A model of re-assembled split-EmCit. The red part of the beta-barrel structure of EmCit symbolizes the N-terminus (NEmCit), green shows the C-terminus (CEmCit). The EmCit gene and thereby also the protein was split into the nonfluorescent NEmCit and CEmCit. EmCit fluorescence can be restored by auto-assembly of the two parts (design rationale: Kerppola, 2006; structure: http://www.rcsb.org/pdb/explore.do?structureId=2y0g; editing: Guanbin Gao). (b) *MAD1* and *MAD2* are tagged with one portion of split-EmCit each. The N-terminus of *MAD1* is linked to *NEmCit* and regulated by the endogenous *MAD1* promoter. The N-terminus of *MAD2* is labled with *CEmCit*. The fusion protein is under the control of a strong *TPI* promoter.

I transformed NEmCit and CEmCit containing plasmids (415-NEmCit-gMad1, 416-Tc-CEmCit-MAD2) into *vps74-1/mad2Δ.* The transformants were treated with benomyl to trigger SAC activation, which initiates a fluorescent signal due to the assembly of split-EmCit (Figure 15, 16). Cycling cells showed some fluorescent parts (arrows), but much less then benomyl-treated cells. Drug-treated cells contained two or more distinctly visible EmCit spots of different intensities. The spots are located in both mother and bud, and little or no co-localization with the DAPI stained nucleus can be observed. Besides,

examined cells did not show the typical shape of cells arrested in late G_2 respectively early M phase.

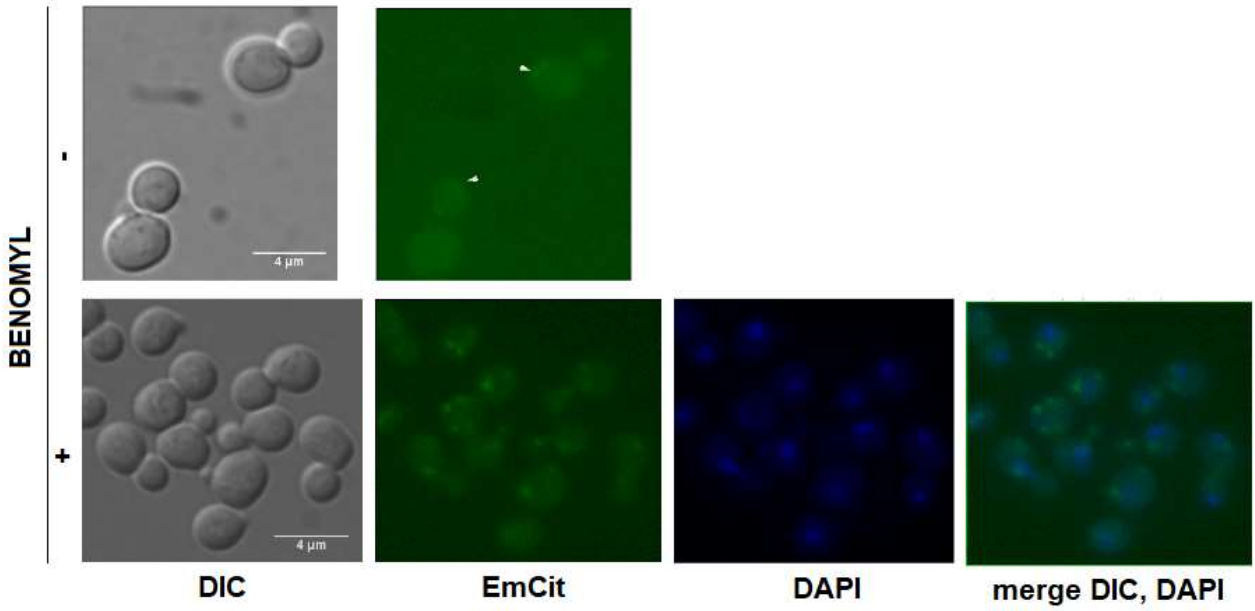

Figure 15: Microscopic images of *vps74-1/mad2Δ* expressing a plasmid-born copy of NEmCit-Mad1 and CEmCit-Mad2 with and without benomyl treatment. Cells were grown until early log phase, harvested and released ether in selective medium or selective medium containing 30 µg/ml benomyl. After 120 min incubation at 25 °C cells were fixated, stained and examined. White arrows show cell parts with higher fluorescence. A spotted pattern of EmCit signal (green) is visible in drug-treated cells. The nucleus is stained with DAPI (blue). Merged DAPI and EmCit images do not show co-localization of nucleus and split-EmCit.

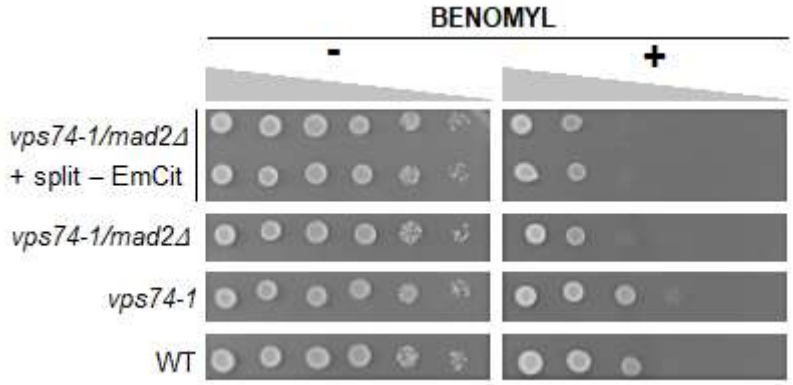

Figure 16: *vps74-1/mad2Δ* expressing a plasmid-born copy of NEmCit-Mad1 and CEmCit-Mad2. Two strains expressing split-EmCit were grown until log phase and spotted on -LEU -URA plates with or without benomyl. Plates were incubated at 25 °C for 2 days. Split-EmCit cannot rescue *vps74-1/mad2Δ* since the transformants are as sensible to benomyl as before transformation.

I spotted two strains expressing split-EmCit on -LEU -URA plates with or without benomyl (Figure 16). Split-EmCit could not restore the decreased benomyl sensitivity of *vps74-1.* Instead, the transformants show the same phenotype as *vps74-1/mad2Δ.* Hence, it is questionable, if drug treatment triggered the signal of EmCit. To test the functionality of NEmCit-Mad1 and CEmCit-Mad2 individual, I transformed *vps74-1/mad2Δ* and *mad2Δ* with 416-Tc-CEmCit-MAD2 or plasmids containing the native form of MAD2 (415-MAD2, 425-MAD2). I also transformed a *MAD1* deletion strain (*mad1Δ*) accordingly with 415-NEmCit-gMad1 or 416-MAD1. Figure 17 shows the transformants spotted on benomyl-containing plates. Interestingly only strains expressing a low copy YCp with a native *MAD* form were able to restore the phenotype of either WT or *vps74-1*. Neither expression of NEmCit-Mad1 nor CEmCit-Mad2 led to SAC activation. The transformation of the strains with empty vectors did not influence benomyl sensitivity.

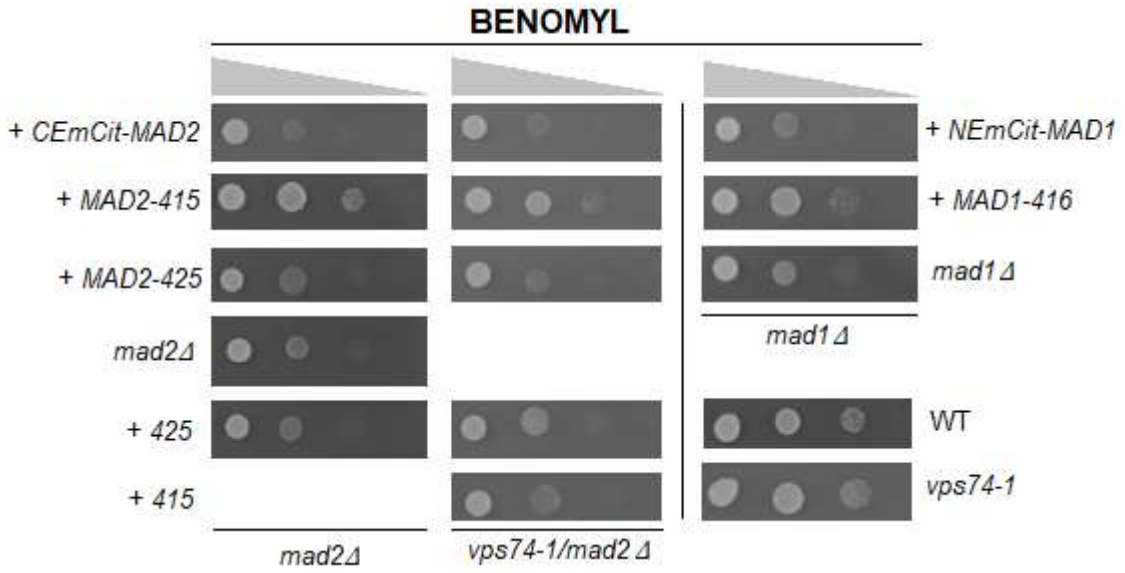

Figure 17: mad2*Δ*, *vps74-1/mad2Δ* and *mad1Δ* expressing plasmid-born copies of CEmCit-Mad2 or NEmCit-Mad1 on benomyl-containing plates. Additionally, strains express plasmid-born copies of unaltered Mad2 in different concentrations *(mad2Δ, vps74-1/mad2Δ*) or Mad1 (*mad1Δ*). All strains were transformed with empty vectors carrying the absent auxotrophic marker (not indicated). Indicated empty vectors serve as a control. Strains were spotted on -LEU -URA plates containing 30 µg/ml benomyl and incubated at 25 °C. Control plates without benomyl are not shown. The depicted experiment can only give the first indication, as essential controls are missing.

4 Discussion

The study attempted the development of a device to visualize the spindle assembly checkpoint activity on single cell level by modification of the spindle assembly checkpoint component Mad2. The suitability of Mad2-EmCit relocation from NPCs (SAC OFF) to unattached kinetochores (SAC ON) as a checkpoint activity marker was examined. Furthermore, I tested the eligibility of split-EmCit to visualize the binding of Mad1 and Mad2.

4.1 Cells are able to express the fusion protein Mad2-EmCit

A *MAD2-EmCit* construct was transformed into the *MAD2* deletion strain *mad2*∆ by homologous recombination. Artificial selection indicated successful transformations. Figure 6b shows the initial situation of *mad2*∆: the strain can grow on G418-containing plates, due to the replacement of *MAD2* by the *KanMX4* marker, which provides G418 resistance. The *MAD2-EmCit-KILEU2* construct enables transformants to grow on -LEU plates. Since *MAD2-EmCit-KILEU2* replaces *KanMX4*, the transformants are not resistant to G418 anymore. The chosen *mad2*∆ + *MAD2-EmCit* strains show G418 sensibility in addition to growths on -LEU plates. I assume, that the transformation was successful and the fragment was located at the expected position in *mad2*∆. This assumption is confirmed by PCR (Figure 6e).

Different methods verified the expression of Mad2-EmCit. In microscopic examinations, cells showed an EmCit fluorescence signal in the nucleus area. Moreover, Mad2-EmCit was detected by anti-GFP antibodies (Figure 7). The large complex could be ascertained for all tested transformants in the range between 37 and 49 kDa. No unbound EmCit was found. The function of Mad2-EmCit was tested by spotting the strains on benomyl-containing plates. The drug inhibits microtubule polymerization; consequently, kinetochores of cells in M phase remain unattached. The mitotic checkpoint needs to be

activated to avoid segregation fails. SAC activation requires Mad2. Therefore chromosome segregation errors are inevitable for *MAD2* deletion strains. Benomyl sensibility is increased in *MAD2* deletion strains, though functional Mad2 can rescue them. The serial dilution tests proofed that Mad2-EmCit can rescue the *mad2*Δ strain (Figure 8). As a conclusion, I assume the expression and correct function of Mad2-EmCit. Placement, expression, and function of the fusion protein were also tested for *vps 74-1/mad2*Δ transformants. Figure 13 shows the restored temperature sensitivity of the *vps74-1* strain. Around 20 transformants were tested. All of them showed decreased benomyl sensitivity, but only two a Ts phenotype. The Mad2-EmCit-expressing *vps74-1/mad2Δ* strain chosen for further tests was unable to grow at 37 °C due to its strong Ts phenotype (Figure 13a). The unmodified Mad2 expressed in *vps74-1/mad2*Δ + MAD2 perfectly restored the Ts phenotype of *vps74-1*. Therefore it is possible, that Mad2-EmCit could be not fully functional.

4.2 Mad2-EmCit expressing cells failed to show clear kinetochore foci

Mad2 was successfully tagged with EmCit. Microscopic studies show the expected association of Mad2-EmCit with the nuclear envelope in cycling cells. Moreover, Mad2-EmCit was able to rescue the *MAD2* deletion strains *mad2Δ* and *vps74-1/mad2Δ* when spotted on benomyl-containing plates. These results suggest the assumption of a functional Mad2-EmCit fusion protein. However, it was not possible to visualize the ON status of SAC by fluorescence microscopy. The cells failed to show the expected strong Mad2-EmCit signal at unattached kinetochores. In the Figures 9 and 10, relatively strong EmCit signals are marked by arrows. It is likely that these spots show focused regions of the nuclear envelope, where Mad2-EmCit is associated with the NPCs.

Mad2-EmCit-expressing cells were exposed to a benomyl-containing medium for 90-120 min to trigger SAC activation. The drug is barely soluble in the water-based cultivation media. Previous studies suggest a benomyl concentration of 30 µg/ml, whereas

Yalkowsky and Dannenfelser reported the maximal solubility of the drug in water as 3.8 µg/ml ((Iouk et al., 2002; Yalkowsky and Dannenfelser, 1992). Benomyl precipitates in water. Therefore it is difficult to determine its final concentration in a medium. Laboratory protocols describe very different procedures of benomyl treatment in liquid cultures and the method is described vaguely in previous studies (Iouk et al., 2002). The method of benomyl-induced cell cycle arrest could be unreliable. Furthermore, in this study cell cycle arrest was detected only by the number of nucleus and cell shape. The estimated share of cells showing these features was unsatisfactorily low in all experiments. A cell cycle arrest was not verified by other methods like fluorescence-activated cell sorting (FACS). One possible reason for the undetectable relocation of Mad2-EmCit to kinetochores in this studies could be a leak of M phase arrested cells. Mad2-EmCit expressing cells spotted on benomyl containing plates activated the SAC, However, samples taken directly from the plates did also not show the expected kinetochore signal.

Different studies showed an observable relocation of tagged Mad2 (Iouk et al., 2002; Gillett et al., 2004; Magiera et al., 2014). In all studies, GFP was used and mostly linked to the C-terminus of Mad2. The C-terminus of the protein is responsible for ligand binding. Nevertheless, placement of the tag at this location seems to be unproblematic. In addition, Mad2 and EmCit were linked by a flexible GAGA linker in this study. Disproportionally negative effects on protein function caused by the design of the fusion protein seem to be unlikely. Indeed, small effects cannot be ruled out, especially in view of the strong Ts phenotype of *vps 74-1/mad2*∆ *+ MAD2-EmCit.*

GFP is a widely used reporter for protein expression, transport, and localization, but has a tendency dimerize (Krasowska et al., 2010). That can lead to difficulties when interacting proteins are tagged with GFP, like the Mad2 intermediates. In some cases, it changed protein localization (Hanson and Ziegler, 2004). Especially the clarity of the Mad2-GFP kinetochore signal reported by Iouk et al. (Figure 4b) could be enhanced by aggregation of the reporter protein. Otherwise, even if that is the case, it may not be important for using tagged Mad2 to determine the status of the mitotic checkpoint. The

correct function and amount of relocated Mad2 are irrelevant as long as Mad2 can activate the SAC if required.

In a study by Iouk et al., published in 2002, the authors confirmed the drug-induced G_2/M arrest of the cells by FACS analysis. However, Mad2-GFP foci were observable in only 50 % of these arrested cells. Moreover, microscopic images of Mad2-GFP in previous studies were highly processed and imaged using z-stacks. Special microscopy equipment and processing skills would be needed to use the weak Mad2-EmCit as checkpoint activity assay. That would be a disadvantage since the observation of Mad2 should be as easy and direct as possible.

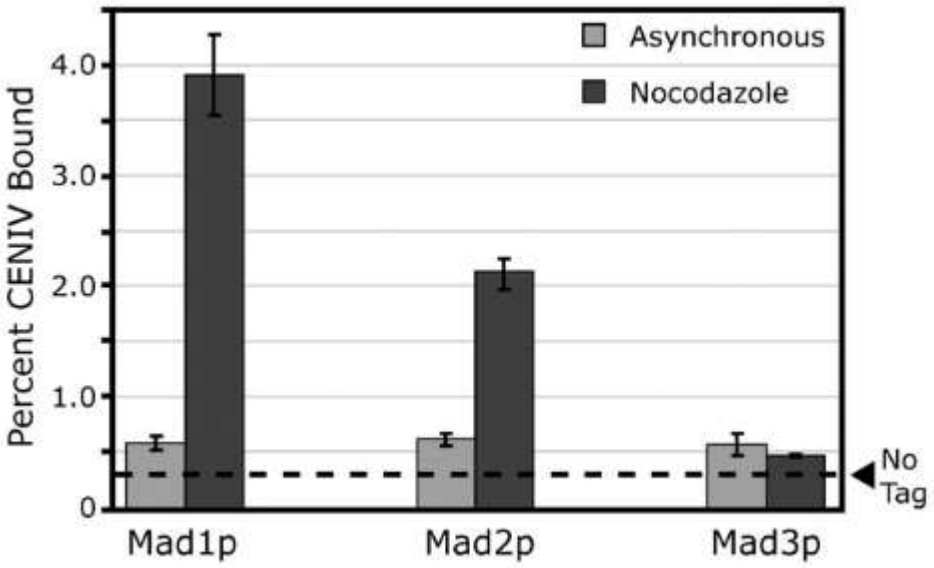

Figure 18: Kinetochore association of GFP tagged Mad1-3 in nocodazole-treated and cycling cells. Shown is the amount of CENIV DNA recovered with immune complexes as a percentage of total CENIV DNA present in cell lysates. The dashed line represents the percentage of recovered CENIV DNA from WT cells as a negative control (From Gillett et al., 2004).

In a study from 2004 by Gillett et al., chromatin immunoprecipitation (ChIP) was used to find out, how much Mad2-GFP binds to unattached kinetochores of chromosome IV after nocodazole treatment (Figure 18). Mad2 binds to CEN DNA via CBF3 complex, required for spindle checkpoint function and assembly of kinetochore components (Gardner et al., 2001; McCleland et al., 2003; McAinsh et al., 2003). For ChIP, kinetochore-bound Mad2-GFP was cross-linked to chromosome IV centromere (CENIV) DNA *in vivo*. The DNA was cut into small fragments, and DNA-protein complexes were isolated using precipitation by anti-GFP antibodies. Depicted is the amount of CENIV recovered with immune complexes as a percentage of the amount of CENIV found in each cell lysate. Mad2-GFP bound around 2 % of CENIV in nocodazole-treated cells. Same to benomyl, nocodazole destabilizes the spindle which leads to some unattached kinetochores. Gillett et al. examined only one chromosome, whose kinetochores were probably attached to microtubules in most cells of the lysate after nocodazole treatment. That could be a reason for the low amount of CENIV bound to Mad2. One possible conclusion could be that drug-induced cell cycle arrest leads to only a few unattached kinetochores. Their signal could be too weak to be detectable, and a more significant number of unattached kinetochores would be needed to observe Mad2 kinetochore foci. However, to keep the SAC active one unattached kinetochore is sufficient. Cells could be arrested by activation of the mitotic checkpoint, even if a kinetochore signal of tagged Mad2 is not observable. That could explain why only a part of arrested cells in previous studies show kinetochore foci.

4.3 Tagged Mad2 is inappropriate to visualize the status of mitotic checkpoint activity

It remains unclear why cells expressing Mad2-EmCit failed to show the expected strong kinetochore foci. Benomyl triggered cell cycle arrest could be insufficient or the microscopy method immature. However, I want to make the general conclusion that the amount of Mad2 bound to a low number of kinetochores could be insufficient to be easily

detected by microscopy. Therefore tagged Mad2 seems to be an inappropriate device to visualize the status of mitotic checkpoint activity.

4.4 Usage of split-EmCit could be a promising method

By utilizing split-EmCit to visualize the binding of Mad1 and Mad2, EmCit foci could be observed after benomyl treatment. Cells contained two or more spots of different intensities located in mother and bud. Overlay of DAPI (nucleus) and EmCit images show little or no co-localization of EmCit-Mad1-Mad2 and the nucleus signal. Beside this, *vps74-1/mad2Δ* expressing split-EmCit from plasmids failed to restore the *vps74-1* phenotype when growing on benomyl-containing plates. Expressing split-EmCit tagged Mad1 and Mad2 did not influence the drug sensitivity. Further tests on benomyl containing plates showed that neither individual expression of NEmCit-Mad1 nor CEmCit-Mad2 in appropriate deletion strains could activate the SAC. Therefore it is possible, that something else than checkpoint activation caused the EmCit foci in benomyl-treated cells. During a regular cell cycle, Mad1 and Mad2 are associated with NPCs (Iouk et al., 2002). This co-localization could lead to a binding of EmCit portions without recruitment to kinetochores. Moreover, the *TPI* promoter regulated expression of Mad2 could lead to difficulties. The strong promoter could cause Mad2 overexpression (Partow et al., 2010). High levels of Mad2 can induce a SAC arrest spontaneously by the formation of Mad2-Cdc20 complexes and recruitment of additional components (Mariani et al., 2012). The sensible interaction of Mad1 and Mad2 plays a key role in SAC activation, wherefore permanent binding of these two proteins could be problematic.

Nevertheless, using split-EmCit could be a promising method to detect SAC activity, but further tests are necessary.

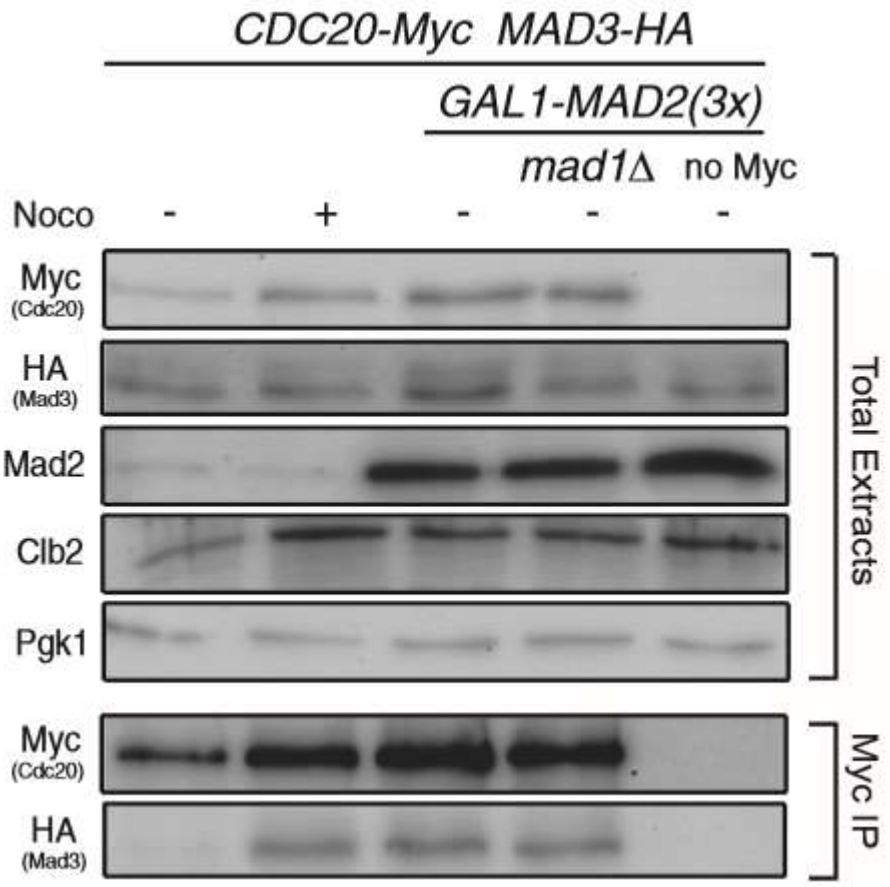

Figure 19: MCC formation induced by Mad2 overexpression and nocodazole treatment. Protein extracts were analyzed by immunoblotting either directly (total extracts) or after Cdc20-Myc immunoprecipitation (Myc IP). Mad3-HA was detectable with anti-HA antibodies after Myc IP, since it formed the MCC together with Cdc20 (From Mariani et al., 2012).

At this point, I want to suggest the following different strategy how to observe SAC activation: In a study by Mariani et al. from 2012, MCC formation and therefore SAC activation was verified by immunoblotting (Figure 19). The MCC components Cdc20 and Mad3 were tagged with Myc respectively hemagglutinin (HA) epitope tags (CDC20-Myc, MAD3-HA). Protein extracts were analyzed either directly by immunoblotting with antibodies (total extracts) or after Cdc20-Myc immunoprecipitation with anti-Myc antibodies (Myc IP). In strains with an active mitotic checkpoint, Mad3-HA was detectable by anti-HA

antibodies after Myc IP. Mad3 and Cdc20 must have formed a complex, the MCC. Observation of SAC activity in a similar way would be not as direct as visualization of the SAC by fluorescent tagged Mad2. The method is inapplicable for studies on a single cell level. However, it could be useful to give an overall image of a strain under different conditions.

4.5 Conclusion

Finally, in this study Mad2 was successfully tagged with EmCit and the fusion protein was observable at the nuclear envelope in cycling cells. Why cells failed to show kinetochore foci after benomyl treatment remains unclear. Possible reasons are inadequate drug-induced cell cycle arrest or an unsuitable microscopy technique. Results of literature search suggest that tagged Mad2 is inapplicable to visualize the activity of the mitotic checkpoint. It appears that the method is not reliable since the weak signal of only a few unattached kinetochores is challenging to detect by microscopy.

Split-EmCit was tested to visualize the protein-protein interaction between Mad1 and Mad2. Even if strains did not show SAC activation on benomyl containing plates, it could be a promising method. It could be worthwhile to test split-EmCit tag on different protein pairs involved in SAC activation in further studies.

Bibliography

Alfieri C., Chang L., Zhang Z., Yang J., Maslen S., Skehel M., Barford D. 2016. Molecular basis of APC/C regulation by the spindle assembly checkpoint. Nature 536:431–436

Cheeseman I. M., Desai A. 2008. Molecular architecture of the kinetochore-microtubule interface. Nat Rev Mol Cell Biol. 9:33–46

Westermann S., Drubin D. G., Barnes G. 2007. Structures and functions of yeast kinetochore complexes. Annu Rev Biochem. ;76:563–91

Meyer R. E., Dawson D. S. 2013 Attaching to spindles before they form: Do early incorrect chromosome-microtubule attachments promote meiotic segregation fidelity? Cell Cycle. 12(13):2011-2015

De Antoni A.,Pearson C. G., Cimini D., Canman J. C., Sala V., Nezi L., Mapelli M., Sironi L., Faretta M., Salmon E. D., Musacchio A. 2005. The Mad1/Mad2 Complex as a Template for Mad2 Activation in the Spindle Assembly Checkpoint. Current Biology 15: 214–225

Gardner R. D., Poddar A., Yellman C., Tavormina P. A., Monteagudo M. C., and Burke D. J. 2001. The spindle checkpoint of the yeast Saccharomyces cerevisiae requires kinetochore function and maps to the CBF3 domain. Genetics. 157:1493–1502.

Gillett E. S., Espelin C. W., Sorger P.K. 2004. Spindle checkpoint proteins and chromosome–microtubule attachment in budding yeast. The Journal of Cell Biology, 164 (4): 535-546

Gorr I. H., Boos D., Stemmann O. 2005. Mutual inhibition of separase and Cdk1 by two-step complex formation. Mol. Cell 19:135–41

Griesbeck O, Baird G. S., Campbell R. E., Zacharias D. A., Tsien R. Y. 2001. Reducing the environmental sensitivity of yellow fluorescent protein. Mechanism and applications. J Biol Chem276: 29 188–29 194.

Guthrie, C. and Fink G. R., Guide to yeast genetics and molecular biology, in Methods in enzymology v 194, 350, 351. 1991, Academic Press, San Diego

Haass, F. A., Jonikas, M., Walter, P., Weissman, J. S., Jan, Y.-N., Jan, L. Y., Schuldiner, M. 2007. Identification of yeast proteins necessary for cell-surface function of a potassium channel. Proceedings of the National Academy of Sciences of the United States of America, 104(46), 18079–18084.

Hanson D. A., Ziegler S. F. 2004. Fusion of green fluorescent protein to the C-terminus of granulysin alters its intracellular localization in comparison to the native molecule. Journal of Negative Results in BioMedicine 3:2

Hara M., Özkan E., Sun H., Yu H., Luo X. 2015. Structure of an intermediate conformer of the spindle checkpoint protein Mad2. PNAS 112, no. 36: 11252–11257

Iouk T., Kerscher O., Scott R. J., Basrai M. A., Wozniak R.W. 2002. The yeast nuclear pore complex functionally interacts with components of the spindle assembly checkpoint. The Journal of Cell Biology, 159 (5): 807–819

Kerppola T. K. 2006. Design and Implementation of Bimolecular Fluorescence Complementation (BiFC) Assays for the Visualization of Protein Interactions in Living Cells. Nat Protoc.1(3): 1278–1286

Krasowska J., Olasek, M., Bzowska A., Clark P. L., Wielgus-Kutrowska B. 2010. The comparison of aggregation and folding of enhanced green fluorescent protein. Spectroscopy 24: 343–348

Lara-Gonzalez P., Westhorpe F. G., Taylor S.S. 2012. The Spindle Assembly Checkpoint. Current Biology 22, R966–R980

Li R., Murray A.W. 1991. Feedback control of mitosis in budding yeast. Cell. 66:519–531. (published erratum in Cell. 1994. 79:following 388)

Li X., and Nicklas R. B. 1995. Mitotic forces control a cell-cycle checkpoint. Nature. 373:630–632.

Magiera M. M., Gueydon E., Schwob E. 2014. DNA replication and spindle checkpoints cooperate during S phase to delay mitosis and preserve genome integrity. The Journal of Cell Biology 204 (2): 165-175

Marczynski G. T., Jaehning J. A. 1985. A transcription map of a yeast centromere plasmid: unexpected transcripts and altered gene expression. Nucleic Acids Research 13 (23): 8487-8506

Mariani L., Chiroli E., Nezi L., Muller H., Piatti S., Musacchio A., Ciliberto A. 2012. Role of the Mad2 Dimerization Interface in the Spindle Assembly Checkpoint Independent of Kinetochores. Current Biology 22: 1900–1908

McAinsh A. D., Tytell J. D., Sorger, P. K. 2003. Structure, function, and regulation of budding yeast kinetochores. Annu. Rev. Cell Dev. Biol. 19:519–539.

McCleland M. L., Gardner R. D., Kallio M. J., Daum J. R., Gorbsky G. J., Burke D. J., Stukenberg P. T. 2003. The highly conserved Ndc80 complex is required for kinetochore assembly, chromosome congression, and spindle checkpoint activity. Genes Dev. 17:101–114.

Miyawaki A., Griesbeck O., Heim R., Tsien R. Y. 1999. Dynamic and quantitative Ca2+ measurements using improved chameleons. Proc Natl Acad Sci USA 96: 2135–2140

Mulla W., Zhu J., Li R. 2014. Yeast: A simple model system to study complex phenomena of aneuploidy. FEMS microbiology reviews 38(2):201-212.

Nasmyth K., Haering C. H. 2009. Cohesin: its roles and mechanisms. Annu. Rev. Genet. 43, 525–558.

Partow S., Siewers V., Bjorn S., Nielsen J., Maury J. 2010. Characterization of different promoters for designing a new expression vector in Saccharomyces cerevisiae. Yeast 27: 955–964

Pines J. 2011. Cubism and the cell cycle: the many faces of the APC/C. Nat. Rev. Mol. Cell Biol. 12, 427–438.

Rieder C. L., Cole R. W., Khodjakov A., Sluder, G. 1995. The checkpoint delaying anaphase in response to chromosome monoorientation is mediated by an inhibitory signal produced by unattached kinetochores. J. Cell Biol. 130, 941–948.

Rieder C.L., Schultz A., Cole R., and Sluder G. 1994. Anaphase onset in vertebrate somatic cells is controlled by a checkpoint that monitors sister kinetochore attachment to the spindle. J. Cell Biol. 127:1301–1310.

Sheff M. A., Thorn K. S. 2004. Optimized cassettes for fluorescent protein tagging in Saccharomyces cerevisiae. Yeast 21, 661-670.

Uhlmann F, Wernic D, Poupart M. A, Koonin E, Nasmyth K. 2000. Cleavage of cohesin by the CD clan protease separin triggers anaphase in yeast. Cell 103:375–86

Xie W., Nielsen M. E., Pedersen C., ThordalChristensen H. 2017. A Split-GFP Gateway Cloning System for Topology Analyses of Membrane Proteins in Plants. PLoS ONE 12(1): e0170118.

Yalkowsky S. H., Dannenfelser R. M. 1992. The Aquasol Database of Aqueous Solubility. Ver 5. Tucson, College of Pharmacy

Zhou J., Yao J., Joshi H. C. 2002. Attachment and tension in the spindle assembly checkpoint. Journal of Cell Science 115: 3547-3555

Hiermit versichere ich, dass ich die vorliegende Masterarbeit erstmalig einreiche, selbständig verfasst und keine anderen als die angegebenen Quellen und Hilfsmittel verwendet habe.

Berlin, den 24.11.2017